Karlsruhe Institute of Technology

Improper Colorings of 1-Planar Graphs

Bachelor's Thesis of

Arian Elias Küpper

At the Department of Informatics
Institute of Theoretical Informatics (ITI)

Reviewer:	PD Dr. Torsten Ueckerdt
Second reviewer:	Prof. Dr. Marvin Künnemann
Advisor:	PD Dr. Torsten Ueckerdt

11/30/2025 – 03/30/2026

Karlsruher Institut für Technologie
Fakultät für Informatik
Postfach 6980
76128 Karlsruhe

The following tools were used to create this thesis:

- Grammarly, for the checking and correction of spelling, punctuation, and grammar. None of the rewriting, text generation, and AI chat functionalities of Grammarly were used.

I declare that I have developed and written the enclosed thesis completely by myself. I have not used any other than the aids that I have mentioned. I have marked all parts of the thesis that I have included from referenced literature, either in their original wording or paraphrasing their contents. I have followed the by-laws to implement scientific integrity at KIT.

Karlsruhe, 03/27/2026

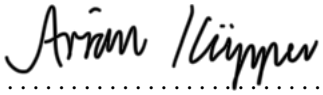

(Arian Elias Küpper)

Abstract

A graph G is called *1-planar* if G can be drawn in the plane so that each edge crosses at most one other edge. A 1-planar graph on n vertices is called *optimal* if it has $4n - 8$ edges, the maximum possible. An *improper coloring* is a coloring of the vertices of a graph so that adjacent vertices may have the same color. A variant of improper coloring is a *c-clustered coloring*, in which all connected components formed by vertices of any single color contain at most c vertices.

We introduce *TQ-embedded graphs*, a subclass of 1-planar graphs for which the uncrossed edges form a planar graph in which every face is bounded by a cycle of length 3 or 4. We study an approach for finding clustered 4-colorings of 1-planar graphs based on deleting and contracting edges to obtain a planar graph and invoking the Four-Color-Theorem. For this approach, we reduce the problem of finding a planarization edge set, that is, a suitable set of edges to delete and contract, from all maximal 1-planar graphs to TQ-embedded graphs.

We discuss several approaches for finding planarization edge sets in TQ-embedded graphs and subclasses of TQ-embedded graphs. Notably, we prove that every optimal 1-planar graph without a separating cycle of length 4 formed by uncrossed edges admits a 10-clustered 4-coloring.

Zusammenfassung

Ein Graph G heißt *1-planar*, wenn es möglich ist, G in der Ebene zu zeichnen, sodass jede Kante höchstens eine andere Kante kreuzt. Ein 1-planarer Graph mit n Knoten heißt *optimal 1-planar*, wenn er $4n - 8$ Kanten hat, die maximal mögliche Anzahl. Eine *unzulässige Färbung* eines Graphen weist jedem Knoten eine Farbe zu und schließt dabei nicht aus, dass benachbarte Knoten dieselbe Farbe erhalten. Eine Variante von unzulässigen Färbungen sind *c-Cluster-Färbungen*. Bei einer solchen Färbung enthält jede Zusammenhangskomponente jedes einfarbigen Teilgraphen höchstens c Knoten.

Wir führen den Begriff der *TQ-eingebetteten Graphen* ein. Dieser beschreibt eine Klasse von 1-planaren Graphen G, für die der planare Graph gebildet aus den ungekreuzten Kanten von G ausschließlich Facetten enthält, deren Rand ein Kreis der Länge 3 oder 4 ist.

Wir untersuchen einen Ansatz zum Konstruieren von Cluster-Färbungen von 1-planaren Graphen mit 4 Farben, der darauf basiert, Kanten zu kontrahieren und zu löschen, bis wir einen planaren Graphen erhalten, auf den wir den Vierfarbensatz anwenden. Wir reduzieren das Problem, für diesen Ansatz eine geeignete Menge an Kanten zum Kontrahieren und Löschen zu finden, von allen maximalen 1-planaren Graphen auf TQ-eingebettete Graphen.

Wir diskutieren eine Reihe von Ansätzen, um solche Kantenmengen für TQ-eingebettete Graphen oder Unterklassen von TQ-eingebetteten Graphen zu konstruieren. Im Zuge dessen beweisen wir, dass jeder optimal 1-planare Graph, der keinen separierenden Kreis der Länge 4, bestehend aus ungekreuzten Kanten, enthält, eine 10-Cluster-Färbung mit 4 Farben besitzt.

Contents

1 Introduction

One of the most famous theorems in graph theory is the Four-Color Theorem, a theorem on planar graphs. A *planar graph* is a graph that can be drawn in the plane without crossing edges. The Four-Color Theorem states that every planar graph can be colored using at most four colors so that no two adjacent vertices have the same color. The problem first appeared in the context of coloring the countries on a map and was publicly mentioned as far back as 1854 [FG54]. It took over a century, until 1976, for the Four-Color Theorem to be correctly proven [AH77 | AHK77].

In 1965, Gerhard Ringel studied a similar coloring problem on maps [Rin65]. Formalized using graphs, the problem is to find a coloring of both the vertices and the faces of a planar graph, where a face is a connected component of the plane in a fixed planar drawing of the graph. In the wanted coloring, no two adjacent vertices and no two adjacent faces have the same color. Furthermore, no face has the same color as any vertex incident to it. In the study of this coloring problem, Ringel introduced the notion of graphs that can be drawn in the plane so that each edge crosses at most one other edge [Rin65]. This class of graphs is now known as *1-planar graphs*.

In 1984, Oleg Borodin proved a result analogous to the Four-Color Theorem for 1-planar graphs: Every 1-planar graph can be colored using at most six colors so that no two adjacent vertices have the same color [Bor84].

This leads us to investigate if it is possible to color every 1-planar graph using four colors if we relax the properties of the coloring. Colorings in which adjacent vertices are permitted to have the same color are called *improper colorings*. Improper colorings have previously been studied for a multitude of graph classes. Refer to the survey by Wood for an overview of results on improper colorings: [Woo18].

Two important types of improper colorings are *clustered colorings* and *defective colorings*. For $c \in \mathbb{N}$, a coloring of the vertices of a graph G is called *c-clustered* if every color class induces a subgraph of G in which all connected components contain at most c vertices. For $d \in \mathbb{N}$, a coloring of the vertices of a graph G is called *d-defective* if every color class induces a subgraph of G with maximum degree at most d. Note that if G is simple, then every c-clustered coloring of G is also a $(c-1)$-defective coloring of G.

Our work focuses on clustered colorings. Specifically, we focus on clustered 4-colorings. Our approach for finding a clustered 4-coloring of a 1-planar graph G is based on deleting and contracting edges from G to obtain a planar graph G'. We call the set P of deleted and contracted edges a *planarization edge set* of G. We obtain a proper 4-coloring of G' from the Four-Color Theorem and propagate the colors along contracted edges to obtain a coloring of G. The clustering of our coloring of G is bounded by the size of the connected components formed by the edges in P. We call the maximum size of the connected components formed by P the *clustering* of P. Thus, the main problem lies in finding planarization edge sets with bounded clustering for all 1-planar graphs.

A tool we frequently use is the planar skeleton. For a 1-planar graph G associated with a fixed 1-planar drawing, the planar skeleton H is the graph obtained from G by deleting all pairs of crossing edges.

1.1 Our Contribution

Our first contribution is a simple result on conditions for the existence of clustered planarization edge sets: In Theorem 3.6, we show that there exists a graph that does not admit a 2-clustered planarization edge set, in other words, a planarization edge set that is a matching.

Traditionally, when studying coloring problems for a graph class $\mathcal{G}$, we consider only the maximal graphs in $\mathcal{G}$, that is, the graphs $G \in \mathcal{G}$ so that $G + uv \notin \mathcal{G}$ for all non-adjacent vertices u, v in G. A problem with this approach for 1-planar graphs is that maximality cannot be tested based on a fixed drawing: There exist 1-planar drawings of non-maximal 1-planar graphs so that no edge can be added to the drawing without losing the 1-planarity of the drawing [Suz20]. Such a drawing is called a *maximal 1-planar embedding*.

We contribute the introduction of a new class of 1-planar drawings for which the planar skeleton has some stronger properties compared to maximal 1-planar embeddings. We call that class *triquadrangular embeddings* or *TQ-embeddings* for short. A 1-planar drawing D is called TQ-embedding if all faces of the corresponding planar skeleton H are bounded by a cycle of length 3 or 4 and D contains a pair of crossing edges within each 4-face of H.

In Theorem 3.12, we reduce the problem of finding planarization edge sets for maximal 1-planar drawings to finding planarization edge sets for TQ-embeddings. Using a conceptually similar reduction, we further reduce the problem from all TQ-embeddings to TQ-embeddings for which the planar skeleton contains no separating triangles in Theorem 4.14.

We also contribute constructions for finding planarization edge sets with bounded clustering for two subclasses of TQ-embeddings. The first one, described in Theorem 4.24, is based on a geometric representation of the planar skeleton. More notably, in Theorem 5.2, we prove the existence of a 10-clustered planarization edge set for all optimal 1-planar graphs without separating cycles of length 4 in the planar skeleton. A 1-planar graph on n vertices is called *optimal* if it has $4n - 8$ edges, the maximum possible.

1.2 Related Work

Generalizations such as 1-planar graphs and other graph classes closely related to planar graphs are known as *beyond-planar* graphs. The class of beyond-planar graphs most closely related to 1-planar graphs is the class of k-planar graphs, which can be drawn in the plane so that each edge crosses at most k other edges [PT97 | Bek20].

Other important classes of beyond-planar graphs include k-quasi-planar graphs, which can be drawn without k pairwise crossing edges [PSS96 | Ack20], fan-planar graphs, which can be drawn so that each edge only crosses edges with a common endpoint [KU22 | BG20], and upward-planar graphs, which are directed acyclic graphs that can be drawn so that no edges cross and all edges go strictly upward [Riv93 | GT95].

One studied aspect of beyond-planar graphs is recognition complexity. For many classes of beyond-planar graphs, including 1-planar graphs, the recognition problem is NP-complete [GB07 | Bin+15 | Hon20]. Other areas of study include edge density, which is linear for many classes of beyond-planar graphs [PT97 | KU22 | Hon20], and approximation schemes for NP-hard optimization problems such as maximum independent set or minimum vertex cover [GB07].

There is a variety of types of improper colorings, many of them based on well-known types of proper colorings. As a generalization of defective colorings, there are $(d_1, ..., d_k)$-colorings, a variant of defective colorings in which separate defects can be specified for each color [SS23].

Other notable examples include defective and clustered variants of list colorings [Woo18], improper acyclic colorings [BSV99], improper frugal colorings [Kan08], and distinguishing colorings [AC96].

Analogous to proper colorings, an intensely studied aspect of improper colorings is the minimization of the number of colors needed to color all graphs of a graph class [Woo18]. For improper colorings, additional constraints such as bounded clustering may be given [Woo18]. Both upper and lower bounds for the number of required colors [Woo18] and algorithmic complexity of finding optimal colorings [Kan08] are studied.

Another algorithmic problem in the context of improper colorings is finding a similar proper coloring for a given improper coloring [JLR15].

Closely related to the topic of this thesis, there are several notable results on improper colorings of 1-planar graphs. Liu and Wood prove that for all $k \in \mathbb{N}$, all k-planar graphs admit a 5-coloring with bounded clustering [LW22]. Song and Sun prove that all 1-planar graphs with girth at least 6 admit a $(1, 1, 1, 1)$-coloring [SS23]. Note that all $(1, 1, 1, 1)$-colorings are 2-clustered. Furthermore, Chu, Sun, and Yue prove that all 1-planar graphs with girth at least 7 admit a $(2, 0, 0, 0)$-coloring [CSY19].

1.3 Outline

In Chapter 2, we introduce the fundamental definitions and lemmas we use throughout this thesis. Sections 2.1, 2.2, and 2.3 contain well-known definitions and facts on colorings, planar graphs, and 1-planar graphs. Among some well-known definitions, Section 2.4 contains the formal definitions of TQ-embeddings and planarization edge sets. Section 2.5 describes two types of geometric graph representations we use in our constructions.

In Chapter 3, we discuss known results on clustered colorings of 1-planar graphs and analyze conditions for the existence of planarization edge sets. Notably, we reduce the problem of finding planarization edge sets to TQ-embeddings in Section 3.1.

In Chapter 4, we analyze the structure of TQ-embedded graphs and discuss various approaches for finding planarization edge sets for TQ-embedded graphs. Sections 4.1 and 4.3 contain approaches based on contact representations of the planar skeleton. In Section 4.2, we reduce the problem of finding planarization edge sets to TQ-embeddings without separating triangles in the planar skeleton.

In Chapter 5, we construct 10-clustered planarization edge sets for all optimal 1-planar graphs without separating 4-cycles in the planar skeleton.

With Chapter 6, we conclude this thesis and give an overview of open problems for future work.

2 Preliminaries

We begin by formally introducing the concepts and definitions we use throughout this thesis.

We use the following standard notation: Let $G = (V, E)$ be a graph. When not explicitly naming the vertex and edge sets in the definition of a graph, we reference the vertex set as $V(G)$ and the edge set as $E(G)$. For $u, v \in V$, we denote an edge joining u and v as uv. We denote the distance between u and v as $\text{dist}(u, v)$. We denote the neighborhood of v as $N(v)$. For $A \subseteq V$, we denote the subgraph of G induced by A as $G[A]$. Let X be a vertex, edge, vertex subset, edge subset, or subgraph of G. Then we denote the graph obtained from G by deleting X as $G - X$.

Let $n, m \in \mathbb{N}$. The names K_n, C_n, and P_n refer to a complete graph, a cycle, and a path on n vertices, respectively. We refer to cycles and paths of length n as n-cycles and n-paths, respectively. Note that P_n is an $(n-1)$-path. For a cycle C and a path P, we denote length of C and P as $||C||$ and $||P||$, respectively. The name $K_{n,m}$ refers to a complete bipartite graph with bipartition sets of sizes n and m.

We state some standard definitions from graph theory.

Definition 2.1 (Simple Graph)**:** *Let G be an undirected graph. The graph G is called* simple *if the following two properties hold.*

(i) G contains no loops, that is, no edges whose two endpoints are equal.

(ii) G contains no multi-edges, that is, between every pair of vertices exists at most one edge.

In the following, the term *graph* always refers to a simple, undirected graph unless explicitly stated otherwise.

Definition 2.2 (Matching)**:** *Let $G = (V, E)$ be a graph. A* matching *is a set $M \subseteq E$ of edges so that for all $v \in V$, M contains at most one edge incident to v.*

Definition 2.3 (k-Connectivity)**:** *Let $G = (V, E)$ be a graph and $k \in \mathbb{N}$. The graph G is called* k-connected *if G has more than k vertices and all graphs obtained from G by removing at most k vertices are connected.*

Definition 2.4 (Separator)**:** *Let $G = (V, E)$ be a graph. A set $S \subseteq V$ of vertices of G is called a* separator *if $G - S$ is disconnected. If the vertices of a separator S form a k-cycle in G, then S is called a* separating k-cycle*. A separating 3-cycle is also called a* separating triangle*.*

Definition 2.5 (Hamilton Cycle, Hamilton Path)**:** *Let G be a graph. A* Hamilton cycle *of G is a cycle that visits every vertex of G. Analogously, a* Hamilton path *of G is a path that visits every vertex of G.*

A common operation on graphs is contracting an edge so its endpoints fuse.

Definition 2.6 (Edge Contraction)**:** *Let $G = (V, E)$ be a graph and $ab \in E$.* Contracting *the edge ab means replacing a and b by a new vertex c, the* contraction vertex*. In all other edges incident to a or b, c replaces the endpoint a or b, respectively. Furthermore, we define edge contractions to remove all duplicate edges created by the aforementioned procedure.*

2.1 Colorings

Colorings are often modeled as functions assigning each vertex a color. However, for our purposes, the following definition is more practical.

Definition 2.7 (Coloring)**:** *Let $G = (V, E)$ be a graph and $k \in \mathbb{N}$. A* k-coloring *of G is a partition $V = \dot{\bigcup}_{i=1}^{k} V_i$ of the vertex set. The sets $V_1, ..., V_k$ are called* color classes*. The coloring is called* proper *if every color class is an independent set. For each color class, the graph $G[V_i]$ induced by the color class is called a* monochromatic subgraph*. The connected components of each monochromatic subgraph are called* monochromatic components*.*

Note that a coloring of a graph induces colorings of all its subgraphs.
Two well-known classes of improper colorings are *defective colorings* and *clustered colorings*.

Definition 2.8 (Defective Coloring)**:** *Let $G = (V, E)$ be a graph, $k \in \mathbb{N}$, $d \in \mathbb{N}_0$, and $V = \dot{\bigcup}_{i=1}^{k} V_i$ a k-coloring of G. The coloring is called* d-defective *if for all monochromatic subgraphs $G[V_i]$, the maximum degree $\Delta(G[V_i])$ is at most d.*

Definition 2.9 (Clustered Coloring)**:** *Let $G = (V, E)$ be a graph, $k, c \in \mathbb{N}$, and $V = \dot{\bigcup}_{i=1}^{k} V_i$ a k-coloring of G. The coloring is called* c-clustered *if all of its monochromatic components contain at most c vertices.*

A generalization of defective colorings allows separate bounds for the defect of each color class.

Definition 2.10 ($(d_1, ..., d_k)$-coloring [SS23])**:** *Let $G = (V, E)$ be a graph, $k \in \mathbb{N}$, $d_1, ..., d_k \in \mathbb{N}_0$, and $V = \dot{\bigcup}_{i=1}^{k} V_i$ a k-coloring of G. The coloring is called* $(d_1, ..., d_k)$-coloring *if for all $i \in \{1, ..., k\}$ we have $\Delta(G[V_i]) \leq d_i$.*

2.2 Planar Graphs

In our work on 1-planar graphs, we often use planar graphs and their well-known structural properties.

Definition 2.11 (Planar Graph)**:** *Let G be a graph. The graph G is called* planar *if G can be drawn in the plane so that no two edges cross each other. Such a drawing is called a* planar drawing *or* planar embedding*. A planar graph associated with a fixed planar drawing is called an* embedded planar graph*.*

Note that formally, vertices in a drawing are represented as singular points. Analogously, the lines representing edges are infinitesimally thin.
In a planar drawing, the edges of a planar graph divide the plane into components. These components are called faces.

Definition 2.12 (Face)**:** *Let G be an embedded planar graph. The connected components of $\mathbb{R}^2$ obtained from the planar drawing of G by removing all points covered by edges or vertices are called* faces*. The number of edge-sides incident to a face is called the* degree *of the face. A face of degree k is called a* k-face*. Exactly one face of each planar drawing is unbounded. This face is called the* outer face*. All other faces are called* inner faces*.*

The faces of an embedded planar graph and the adjacencies between the faces can be modeled as another graph: the dual graph.

Definition 2.13 (Dual Graph)**:** *Let $G = (V, E)$ be an embedded planar graph. Let F be the set of faces of G. For an edge $e \in E$ with faces $f_1, f_2 \in F$ on its left and right side, respectively, we define the* dual edge *$e^* = f_1 f_2$. The* dual graph *of G is a graph $G^* = (V^*, E^*)$ such that $V^* = F$ and $E^* = \{e^* \mid e \in E\}$. The graph G is called the* primal graph *of G^*.*

Note that the dual of a simple planar graph is not necessarily simple. It is, however, always planar.

Lemma 2.14: *Let G be an embedded planar graph. The dual graph G^* is planar.*

Proof. We obtain a planar drawing of G^* from the planar drawing of G. Draw each vertex of G^* into its corresponding face in G. Then draw each dual edge so that it crosses its corresponding primal edge. ∎

We remark that if the primal graph G is connected, then G is the dual of the dual graph G^*, that is, $G = (G^*)^*$.

The following formula describes a well-known relation between the number of vertices, edges, and faces of connected planar graphs.

Proposition 2.15 (Euler's Formula)**:** *Let $G = (V, E)$ be an embedded connected planar graph. Let F be the set of faces of G. Then $|V| - |E| + |F| = 2$.*

The following bound on the number of edges in a planar graph is a consequence of Euler's Formula.

Proposition 2.16: *If $G = (V, E)$ is an embedded planar graph such that $|V| \geq 3$, then the inequality $|E| \leq 3 \cdot |V| - 6$ holds.*

One of the most famous theorems on planar graphs is the Four-Color Theorem.

Theorem 2.17 (Four-Color Theorem; Appel and Haken, 1976 [AH77 | AHK77])**:** *Every planar graph admits a proper 4-coloring.*

2.3 1-Planar Graphs

The graph class we research, 1-planar graphs, is a special case of k-planar graphs.

Definition 2.18 (k-Planar Graph)**:** *Let $G = (V, E)$ be a graph. The graph G is called* k-planar *if G can be drawn in the plane so that each edge crosses at most k other edges. Such a drawing is called a* k-planar drawing*,* k-planar embedding*, or* k-embedding*. A k-planar graph associated with a fixed k-planar drawing is called an* embedded k-planar graph *or* k-embedded graph*.*

In the following, when considering a subgraph H of an embedded k-planar graph G, we consider the drawing of H induced by the drawing of G.

In the following, without loss of generality, we consider only 1-planar embeddings with the following properties [CH13]:

- No edge crosses itself.
- No two edges cross in multiple points.
- Edges sharing an endpoint never cross.

Another useful property that some 1-planar embeddings have is the following.

Definition 2.19 (Well-Embedding)**:** *Let $G = (V, E)$ be an embedded 1-planar graph and let D be the embedding. The embedding D is called a* well-embedding *if for all $e \in E$, it is not possible to redraw only e in D to obtain a 1-planar embedding of G with fewer crossings than D. If D is a well-embedding, then G is called* well-embedded*.*

Analogous to planar graphs, the number of edges in a 1-planar graph adheres to the following bound.

Proposition 2.20 (see [Suz20])**:** *If $G = (V, E)$ is an embedded 1-planar graph such that $|V| \geq 3$, then the inequality $|E| \leq 4 \cdot |V| - 8$ holds.*

A result similar to the Four-Color Theorem on planar graphs exists for 1-planar graphs. Borodin first proved it in a 1984 paper in Russian [Bor84]. In 1995, he published an updated proof of a special case in English [Bor95].

Proposition 2.21 (Six Color Theorem; Borodin, 1984 [Bor84 | Bor95])**:** *Every 1-planar graph admits a proper 6-coloring.*

For 1-planar graphs, multiple notions of maximality exist. We introduce three of them: Maximal 1-embeddings, maximal 1-planar graphs, and optimal 1-planar graphs.

Definition 2.22 (Maximal 1-Embedding)**:** *Let G be an embedded 1-planar graph and let D be the embedding. The embedding D is called a* maximal 1-embedding *if all drawings obtained from D by drawing a new edge joining previously nonadjacent vertices are not 1-planar. If D is a maximal 1-embedding, G is called a* maximally 1-embedded graph*.*

Definition 2.23 (Maximal 1-Planar Graph)**:** *Let G be a 1-planar graph. The graph G is called maximal 1-planar if all graphs obtained from G by adding an edge are not 1-planar.*

Definition 2.24 (Optimal 1-Planar Graph)**:** *Let $G = (V, E)$ be a 1-planar graph such that $|V| \geq 3$. The graph G is called* optimal 1-planar *if $|E| = 4 \cdot |V| - 8$.*

We remark that there are maximally 1-embedded graphs that are not maximal 1-planar and maximal 1-planar graphs which are not optimal (see, for example, [Suz20], [CH13]).

For optimal 1-planar graphs, the following relationship between the number of vertices and the number of crossings holds.

Proposition 2.25 (Czap and Hudák, 2013 [CH13])**:** *Let $G = (V, E)$ be an optimal 1-planar graph. All 1-planar drawings of G contain exactly $|V| - 2$ crossings.*

Next, we show that in maximally 1-embedded graphs, for all pairs of crossing edges, the endpoints of the crossing edges form a 4-cycle.

Lemma 2.26 (see, e.g., [Suz10])**:** *Let G be a 1-embedded graph. Let ac and bd be a pair of crossing edges in G.*

If G is maximally 1-embedded, then G contains the edges ab, bc, cd, and da.

If G is well-embedded, then for each of the edges ab, bc, cd, and da, if the edge exists, it is uncrossed.

Proof. As ac and bd cross each other, no other edge crosses either of them. Thus, it is possible to draw the edges ab, bc, cd, and da without introducing new crossings by routing them along ac, bd, and the crossing point of ac and bd (see Figure 2.1). For a maximal 1-embedding, this possibility implies the existence of ab, bc, cd, and da. For a well-embedding, this possibility implies that all existing edges of ab, bc, cd, and da are uncrossed. ∎

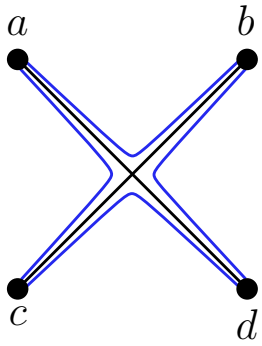

Figure 2.1: For a pair of crossing edges ac and bd, it is possible to draw the edges ab, bc, cd, and da without introducing crossings by routing them along ac, bd, and their crossing point.

2.4 Planarization of 1-Planar Graphs

There are several ways to obtain planar graphs from 1-planar graphs. We present three of them: the associated planar graph, the planar skeleton, and the planarization edge set.

Definition 2.27 (Associated Planar Graph [SS23])**:** *Let $G = (V, E)$ be an embedded 1-planar graph. The* associated planar graph *G^x is obtained from G as follows. For each pair of crossing edges ac and bd, add a new vertex z. Then replace ac and bd with az, bz, cz, and dz.*

The vertices of G^x that exist in G are called true vertices*. The vertices of G^x that originate from eliminating crossing points are called* cross-vertices*.*

Definition 2.28 (Planar Skeleton)**:** *Let G be an embedded 1-planar graph. The embedded planar graph obtained from G by deleting all pairs of crossing edges is called the* planar skeleton *of G.*

We define a subclass of embedded 1-planar graphs based on properties of the planar skeleton: TQ-embedded graphs. TQ-embedded graphs are of particular interest, as we reduce the problem of finding planarization edge sets to TQ-embedded graphs in Theorem 3.12.

Definition 2.29 (TQ-Embedding)**:** *Let G be an embedded 1-planar graph and let D be the embedding. The embedding D is called a* triquadrangular embedding (TQ-embedding) *if the planar skeleton H of G with respect to D contains only 3- and 4-faces, every face of H is bounded by a cycle, and for every 4-face f of H, the graph G contains a pair of crossing edges within f. If D is a TQ-embedding, G is called a* TQ-embedded graph*.*

We introduce a way of planarizing well-embedded 1-planar graphs that is closely related to clustered 4-colorings.

Definition 2.30 (Planarization Edge Set)**:** *Let $G = (V, E)$ be an embedded 1-planar graph.*

A planarization edge set *of G is a set of edges $P \subseteq E$ that* hits *all pairs of crossing edges in G, that is: For each pair of crossing edges $ac, bd \in E$, the set P contains at least one of the edges ac, bd, ab, bc, cd, and da.*

Let $G_P = (V, P)$ be the subgraph of G containing exactly the edges in P. The connected components of G_P are called clusters *of P. Let $c \in \mathbb{N}$. The set P is called c-*clustered *if all clusters of P contain at most c vertices.*

The maximum degree $\Delta(G_P)$ is called the maximum degree *of P. The maximum $l \in \mathbb{N}$ so that G_P contains a path of length l is called the* maximum path length *of P.*

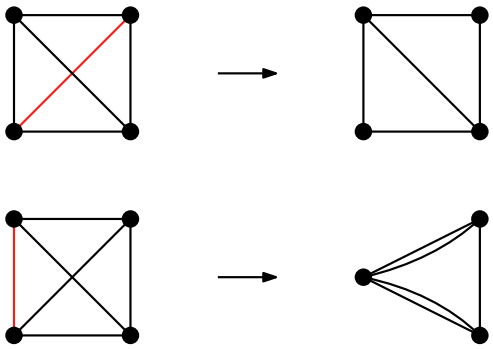

Figure 2.2: Planarization via edge deletion and via edge contraction. For clarity, we show the multi-edges created by the edge contraction before they are deduplicated.

For TQ-embedded graphs, we frequently use the following equivalent characterization of planarization edge sets, which immediately follows from the definitions.

Lemma 2.31: *Let $G = (V, E)$ be a TQ-embedded graph, and let H be the planar skeleton of G. An edge set $P \subseteq E$ is a planarization edge set of G if and only if for all 4-faces f of H, the set P contains an edge from the boundary of f or an edge from G within f.*

If P is a planarization edge set, we say that P hits *all 4-faces of the planar skeleton.*

Planarization edge sets yield the following way of planarizing 1-planar graphs.

Lemma 2.32: *Let G be a well-embedded 1-planar graph and P a planarization edge set of G. The graph obtained from G by contracting all uncrossed edges in P and deleting all crossed edges in P is planar.*

Proof. Let $e \in P$ be an edge hitting the pair of crossing edges ac and bd from G. If e is ac or bd, then e is crossed, and deleting e removes the crossing. If e is one of ab, bc, cd, and da, then e is uncrossed by Lemma 2.26. Contracting e removes the crossing (see Figure 2.2).

Although 1-planar graphs are not closed under edge contraction [Woo18], contracting an uncrossed edge is possible without creating new crossings: Place the contraction vertex along the contracted edge and route the edges incident to the contraction vertex from their former endpoints to the contraction vertex along the contracted edge (see Figure 2.3). ∎

The following lemma breaks the problem of finding clustered planarization edge sets down into two subproblems.

Lemma 2.33: *Let $\mathcal{G}$ be a subclass of 1-planar graphs. If all $G \in \mathcal{G}$, for some 1-embedding, admit a planarization edge set with both bounded maximum degree and bounded maximum path length, then all $G \in \mathcal{G}$ admit a c-clustered planarization edge set for some $c \in \mathbb{N}$.*

Proof. Let Δ be the bound on the maximum degree and L the bound on the maximum path length. Consider any $G \in \mathcal{G}$ and a planarization edge set P of G that adheres to these bounds.

Let C be any connected component of $G_P = (V, P)$. Consider a spanning tree T of C. The height of T is at most L, and each vertex of T has at most Δ children. Thus, T contains at most $c := \sum_{i=0}^{L} \Delta^i$ vertices. ∎

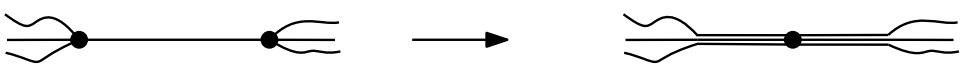

Figure 2.3: Contracting an uncrossed edge produces no new crossing.

2.5 Contact Representations

Geometric representations of graphs are a useful tool for finding planarization edge sets. They allow us to see structures that have no intuitive interpretation in the graph itself. Furthermore, geometric representations provide an elegant way of making use of structural properties of the graphs we analyze.

Contact representations represent vertices of a graph as non-overlapping geometric objects and edges of a graph as contacts between these geometric objects.

2.5.1 Primal-Dual Triangle Representation

One geometric representation we use is a representation by triangles. To describe it, we need to introduce some terminology from [GLP12]:

Definition 2.34 (Primal-Dual Triangle Representation [GLP12])**:** *Let $G = (V, E)$ be an embedded planar graph, $G^* = (V^*, E^*)$ its dual, and f_∞ the outer face of G.*

A triangle representation *of G is a set of non-overlapping triangles with one triangle t_v for each vertex $v \in V$. The triangles have the property that for all $u, v \in V$, we have $t_u \cap t_v \neq \emptyset$ if and only if $uv \in E$.*

A primal-dual triangle representation *is a pair of non-overlapping triangle representations T and T^*, one for the primal graph and one for the dual graph. The representation T^* is slightly modified. Instead of a filled triangle, t_{f_∞} consists of only the boundary of a triangle. Furthermore, the representations have the following property: For all $uv \in E$ with corresponding dual edge $xy \in E^*$, we have $t_u \cap t_v = t_x \cap t_y$.*

We call triangles from T primal triangles*, and we call triangles from T^** dual triangles*.*

A primal-dual triangle representation is called strict *if exactly three triangle corners touch each contact point.*

A primal-dual triangle representation is called tiling *if t_{f_∞} is tiled by the other triangles.*

See Figure 2.4 for an example of a strict tiling primal-dual triangle representation.

In the following, the term *triangle representation* always refers to a strict tiling primal-dual triangle representation.

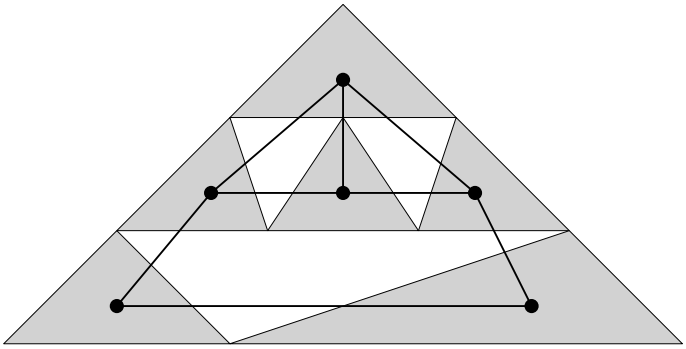

Figure 2.4: Example of a triangle representation with the represented planar graph drawn in. Gray triangles are primal triangles, white triangles are dual triangles. Note that the outer face corresponds to the unbounded area tiled by the other triangles.

To give a condition for the existence of triangle representations, we introduce a concept closely related to 3-connectivity.

Definition 2.35 (Internal 3-connectivity [GLP12])**:** *Let $G = (V, E)$ be an embedded planar graph. The graph G is called* internally 3-connected *if there exist distinct vertices $v_1, v_2, v_3 \in V$ on the outer face of G so that the graph obtained from G by adding a new vertex adjacent to exactly v_1, v_2 and v_3 is 3-connected.*

Note that all 3-connected planar graphs are internally 3-connected [GLP12].

Gonçalves et al. prove that a triangle representation exists for all internally 3-connected planar graphs [GLP12].

Proposition 2.36 (Gonçalves, Lévêque, and Pinlou, 2012 [GLP12])**:** *Each internally 3-connected planar graph admits a strict tiling primal-dual triangle representation.*

A useful property of triangle representations is that we can classify the sides of the triangles as bases, left sides, and right sides. We can also classify the corners of triangles as tips, left corners, and right corners so that each tip only touches the base, each left corner only touches the right side, and each right corner only touches the left side of the adjacent triangle of the same type (primal or dual).

To motivate this, we introduce a structure closely related to triangle representations: Schnyder woods. Specifically, rather than the original variant defined by Schnyder [Sch89], we use a generalized version of Schnyder woods first introduced by Felsner [Fel01].

Definition 2.37 (Schnyder Wood)**:** *The following description is sourced from [GLP12].*

Let G be an embedded internally 3-connected planar graph. Let $v_0, v_1, v_2 \in V$ be three distinct vertices on the boundary of the outer face in clockwise order. The suspension G^σ *is the graph obtained from G by adding a half-edge reaching into the outer face to each of v_0, v_1, and v_2.*

A Schnyder wood *of G consists of a fixed choice of v_0, v_1, and v_2, as well as an orientation and 3-coloring of the edges of G^σ. The edge coloring has the following properties. Let $0, 1$, and 2 be the three colors. We refer to colors in modulo 3.*

- *Each edge is either directed in one direction or bidirected.*
- *If an edge is bidirected, the edge has distinct colors for both directions.*
- *The half-edge at v_i is directed outwards and has color i.*
- *Every vertex $v \in V$ has exactly one outgoing edge $e_i(v)$ per color i. The edges $e_1(v), e_2(v)$, and $e_3(v)$ appear in clockwise order around v.*
- *At every vertex $v \in V$, all ingoing edges of color i appear in the clockwise angle from $e_{i+1}(v)$ to $e_{i-1}(v)$.*
- *No inner face of G has a monochromatic directed cycle as its boundary.*

Figure 2.5 visualizes the coloring and orientation rules of Schnyder woods. Furthermore, it provides an example of a Schnyder wood.

Gonçalves et al. prove the following correspondence between Schnyder woods and triangle representations.

Proposition 2.38 (Gonçalves, Lévêque, and Pinlou, 2012 [GLP12])**:** *Let G be an embedded internally 3-connected planar graph. The non-isomorphic strict tiling primal-dual triangle representations of G are in bijection with the Schnyder woods of G.*

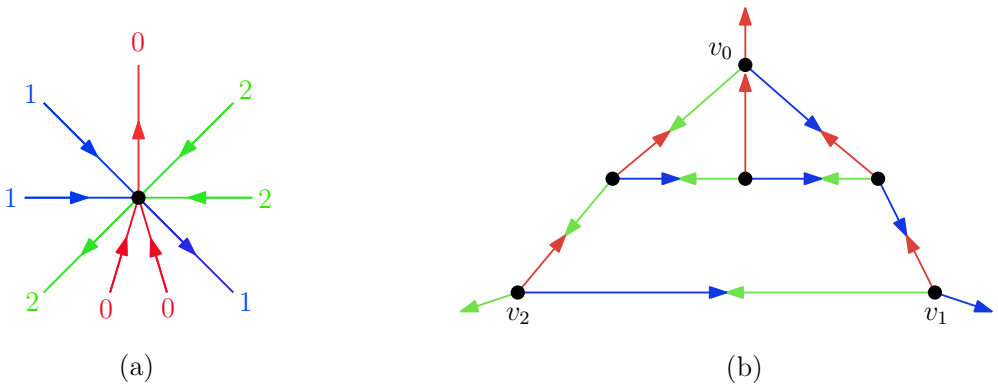

Figure 2.5: (a) Coloring and orientation rules of Schnyder woods around a vertex. (b) Schnyder wood corresponding to the triangle representation in Figure 2.4

Gonçalves et al. describe the relationship between a triangle representation T of a graph $G = (V, E)$ and the corresponding Schnyder wood S as follows. Let $v \in V$ be a vertex of G and let t be the triangle that represents v in T. The outgoing edges $e_1(v), e_2(v)$, and $e_3(v)$ correspond to the corners of t [GLP12]. Furthermore, the angles between $e_1(v), e_2(v)$, and $e_3(v)$ correspond to the sides of t [GLP12]. Furthermore, if an edge $xy \in E$ is bidirected in S, that corresponds to a corner contact between the triangles representing x and y in T [GLP12]. Figures 2.4 and 2.5 provide an example of the relationship between a triangle representation and its corresponding Schnyder wood.

Thus, the edge colors from the Schnyder wood of a triangle representation yield the aforementioned classification of sides and corners. The rules defining Schnyder woods guarantee that the incidence rules we require for our classification are fulfilled. In the following, without loss of generality, we assume all bases of triangles to be horizontal and all tips of triangles to be above (primal triangles) or below (dual triangles) their respective bases.

The classification of triangle sides and corners allows us to classify the contact points of a triangle representation as depicted in Figure 2.6. We classify each contact point p based on the type of the triangle t whose side p touches and which side of t the point p touches.

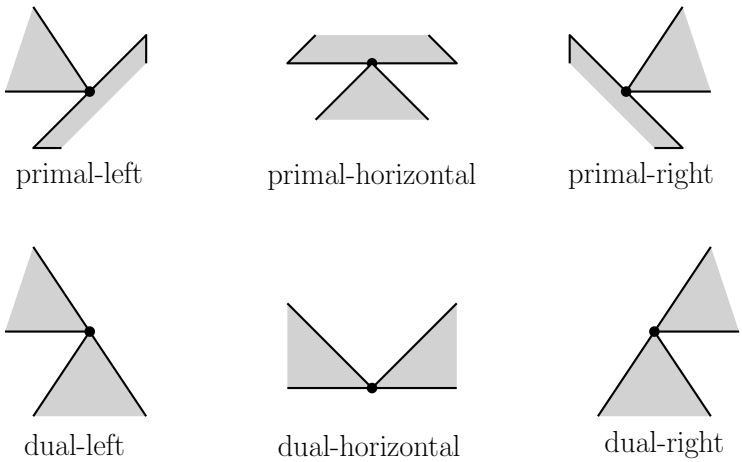

Figure 2.6: The types of contact points in the triangle representation.

Schnyder woods and thus, triangle representations of a graph G are generally not unique. As a tool for choosing and modifying triangle representations, we introduce another structure. It consists of an auxiliary graph A and an orientation of the edges of A. Felsner previously studied these auxiliary graphs and orientations in [Fel04].

In the following, we introduce a slightly simplified version compared to Felsner.

Definition 2.39 (Auxiliary Graph, based on Felsner [Fel04])**:** *Let $G = (V, E)$ be an embedded internally 3-connected planar graph.*

Let f_∞ be the outer face of G. We choose a tuple $(v_1, v_2, v_3) \in V^3$ of three distinct vertices on the boundary of f_∞ in clockwise order.

We define the auxiliary graph $\mathrm{Aux}(G, (v_1, v_2, v_3))$ *of G and our choice of (v_1, v_2, v_3).*

The vertices, edges, and faces of the G are vertices of $\mathrm{Aux}(G, (v_1, v_2, v_3))$.

Edges of $\mathrm{Aux}(G, (v_1, v_2, v_3))$ *connect vertices and faces of G to the edge-vertices corresponding to their incident edges in G.*

For $i \in \{0, 1, 2\}$ we create a new special vertex s_i in $\mathrm{Aux}(G, (v_1, v_2, v_3))$ *adjacent to v_i and f_∞.*

Formally, $\mathrm{Aux}(G, (v_1, v_2, v_3))$ *is a graph so that:*

$$V(Aux(G, (v_1, v_2, v_3))) = V \cup V^* \cup E \cup \{s_0, s_1, s_2\}$$
$$E(Aux(G, (v_1, v_2, v_3))) = \{ae, be \mid e \in E, e = ab\}$$
$$\cup \{ae^*, be^* \mid e^* \in E^*, e^* = ab\}$$
$$\cup \{v_0s_0, v_1s_1, v_2s_2, s_0f_\infty, s_1f_\infty, s_2f_\infty\}$$

We call the vertices of $\mathrm{Aux}(G, (v_1, v_2, v_3))$ *in V and V^** triangle-vertices*, and we call the remaining vertices of* $\mathrm{Aux}(G, (v_1, v_2, v_3))$*, including the special vertices,* edge-vertices.

In the following, when the choice of (v_0, v_1, v_2) is irrelevant or clear from context, we omit it from the notation of the auxiliary graph.

Figure 2.7 shows the auxiliary graph of K_3.

Definition 2.40 (s-orientation, based on Felsner [Fel04])**:** *Let $G = (V, E)$ be an embedded internally 3-connected planar graph. An* s-orientation *of G is an orientation of* $\mathrm{Aux}(G, (v_1, v_2, v_3))$ *for a fixed choice of (v_1, v_2, v_3) so that:*

$$\forall v \in V \cup (V^* \backslash \{f_\infty\}) : outdeg(v) = 3$$
$$\forall e \in E : outdeg(e) = 1$$
$$\forall i \in \{0, 1, 2\} : outdeg(s_i) = 1$$
$$outdeg(f_\infty) = 0$$

The vertices s_0, s_1, and s_2 refer to the special vertices of $\mathrm{Aux}(G, (v_1, v_2, v_3))$.

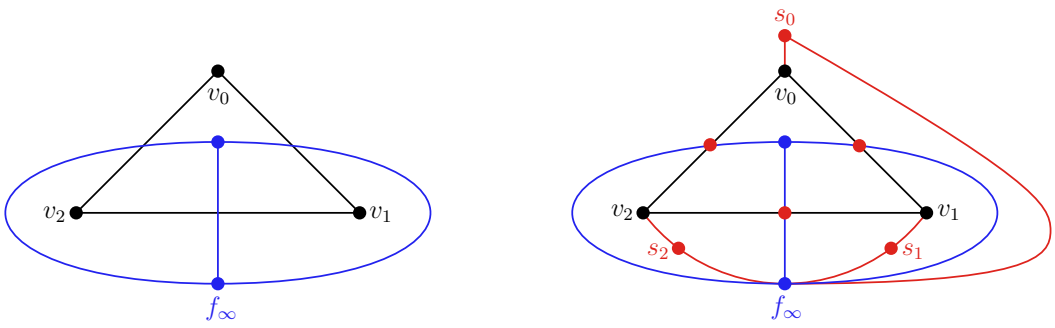

(a) (b)

Figure 2.7: (a) K_3 (black) and its dual graph (blue). (b) Auxiliary graph of K_3

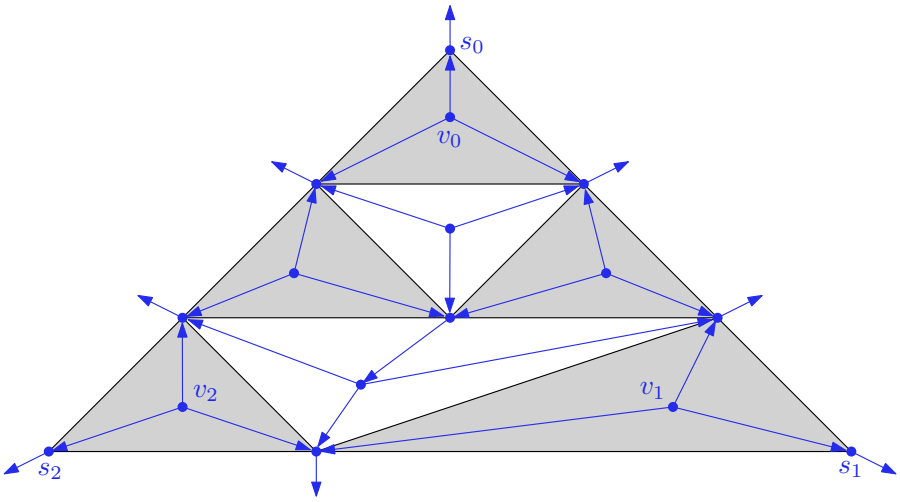

Figure 2.8: Drawing of Aux(G) and the s-orientation associated with a triangle representation. The unbounded area represents f_∞.

Gonçalves et al. prove the following correspondence between s-orientations and triangle representations.

Proposition 2.41 (Gonçalves, Lévêque, and Pinlou, 2012 [GLP12])**:** *Let G be an internally 3-connected planar graph. The non-isomorphic strict tiling primal-dual triangle representations of G are in bijection with the s-orientations of G.*

Gonçalves et al. also describe the relationship between the triangle representation T of a graph G, the s-orientation corresponding to T, and the planar drawing of Aux(G):

We draw the vertices of Aux(G) that represent vertices or inner faces of G within their corresponding triangle [GLP12]. We draw the vertices of Aux(G) that represent edges of G at their corresponding contact point [GLP12]. Let t_1, t_2, and t_3 be the triangles at the tip, right corner, and left corner of T [GLP12]. The triangles t_1, t_2, and t_3 correspond to the vertices v_0, v_1, and v_2, respectively [GLP12]. We draw the special vertices s_0, s_1, s_2 at the outwards-pointing corner of t_1, t_2, t_3, respectively [GLP12].

Then, for each triangle t, the three edges to the corners of t are outgoing, while the edges to all contact points along the sides of t are ingoing [GLP12]. All contact points along the boundary of T have an edge directed to f_∞ [GLP12]. Refer to Figure 2.8 for a visualization.

We define the term *cycle of the triangle representation* to refer to a directed cycle in the corresponding s-orientation.

Given the planar drawing of Aux(G) obtained from T, the directed cycles of an s-orientation can be classified as clockwise or counterclockwise. Reversing the edge directions along a directed cycle does not change the in- and outgoing degrees of any vertex. Thus, reversing directed cycles in Aux(G) allows us to transition between different triangle representations of G due to Proposition 2.41. Figure 2.9 depicts an example of such a reversal of a directed cycle.

Felsner proves a result we can specialize to obtain a useful property of s-orientations:

Proposition 2.42 (Specialized from Felsner, 2004 [Fel04])**:** *Let G be an embedded internally 3-connected planar graph with a triangle representation T. Consider the planar drawing of* Aux(G) *associated with T. Then there is an s-orientation S of* Aux(G) *so that every directed cycle in S is clockwise. Such an s-orientation is called* minimal.

We also call the triangle representation corresponding to a minimal s-orientation *minimal*.

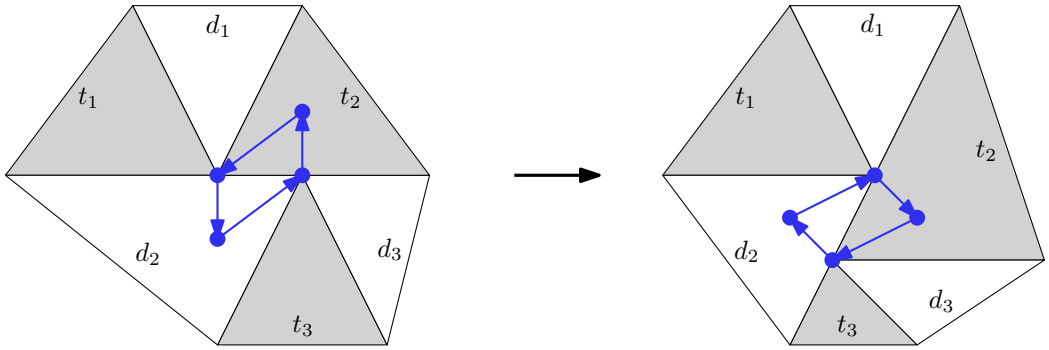

Figure 2.9: Example of a reversal of a counterclockwise cycle in a triangle representation.

2.5.2 Rectangular Dual

Another geometric representation we use is the rectangular dual. It is a contact representation by rectangles.

Definition 2.43 (Rectangular Dual [He93])**:** *Let $G = (V, E)$ be a connected planar graph. The* rectangular dual *represents each vertex of G as a rectangle so that no four rectangles meet at a single point. Together, all rectangles representing vertices tile a single, larger rectangle.*

The rectangular dual represents each edge of G as a side contact of the rectangles corresponding to the edges' endpoints.

Figure 2.10 gives an example of a rectangular dual.

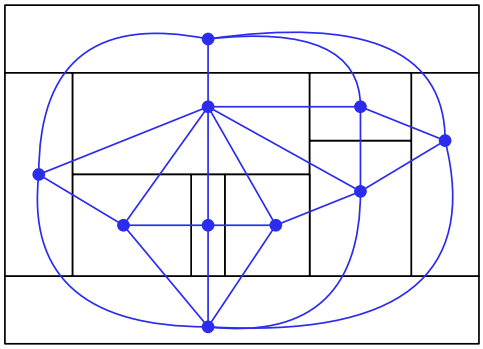

Figure 2.10: Rectangular dual with the represented graph drawn in.

Koźmiński and Kinnen prove a result implying the following condition for the existence of a rectangular dual:

Proposition 2.44 (He, 1993 [He93]; based on Koźmiński and Kinnen, 1985 [KK85])**:** *A connected planar graph G admits a rectangular dual with four rectangles on the boundary if and only if:*

(i) the outer face of G is a quadrangle

(ii) all inner faces of G are triangles

(iii) G contains no separating triangle

Some rectangular duals have the following useful property.

Definition 2.45 (Pierceability)**:** *Let G be a graph with a rectangular dual D. The rectangular dual D is called* pierceable *if the diagonal from the bottom-left to the top-right corner of D intersects the interior of every rectangle in D that represents a vertex from G.*

We remark that graphs exist that admit a rectangular dual, but no pierceable rectangular dual [Uec].

3 General 1-Planar Graphs

In this chapter, we discuss approaches for finding c-clustered n-colorings of 1-planar graphs for a constant c. Specifically, we discuss the case $n = 4$, as it is the only case in which the question of the existence of c-clustered colorings for all 1-planar graphs is open: For $n = 6$, we have the Six-Color Theorem (see Proposition 2.21).

Furthermore, Liu and Wood solved the problem for $n = 5$ for all k-planar graphs.

Proposition 3.1 (Liu and Wood, 2022 [LW22])**:** *For all $k \in \mathbb{N}$, there exists $c \in \mathbb{N}$ so that every k-planar graph admits a c-clustered 5-coloring.*

We remark that the result by Liu and Wood is only available as a preprint at the time of writing.

The following result on planar graphs provides a lower bound for the required number of colors to color k-planar graphs, including 1-planar graphs, with bounded clustering.

Proposition 3.2 (see [Woo18])**:** *For all $c \in \mathbb{N}$, there exists a planar graph that does not admit a c-clustered 3-coloring.*

Regarding $n = 4$, a result by Song and Sun implies the existence of 2-clustered 4-colorings for all 1-planar graphs with girth at least 6.

Proposition 3.3 (Song and Sun, 2023 [SS23])**:** *All 1-planar graphs with girth at least 6 are $(1, 1, 1, 1)$-colorable.*

Note that K_6 is 1-planar. Thus, if $c \in \mathbb{N}$ and $d, l \in \mathbb{N}_0$ exist so that all 1-planar graphs admit a c-clustered 4-coloring, a d-defective 4-coloring, and a 4-coloring with all monochromatic paths having length at most l, respectively, then $c \geq 2, d \geq 1$, and $l \geq 1$.

Our approaches for finding clustered 4-colorings are based on finding planarization edge sets and invoking the following lemma.

Lemma 3.4: *Let $G = (V, E)$ be a well-embedded 1-planar graph and $c \in \mathbb{N}$. If G admits a c-clustered planarization edge set, then G admits a c-clustered 4-coloring.*

Proof. Let P be a c-clustered planarization edge set of G. Let $G_P = (V, P)$ be the subgraph of G containing the edges in P.

Planarize G as described in Lemma 2.32 to obtain a planar graph G'. By the Four-Color Theorem, G' admits a proper 4-coloring.

One by one, we undo each edge contraction performed during planarization and color both endpoints of each contraction edge using the color of the corresponding contraction vertex. This yields a 4-coloring of G.

As the 4-coloring of G' is proper, all edges joining vertices of the same color in G are in P. Thus, each monochromatic component is contained in some connected component of G_P. Therefore, the coloring of G is c-clustered. ∎

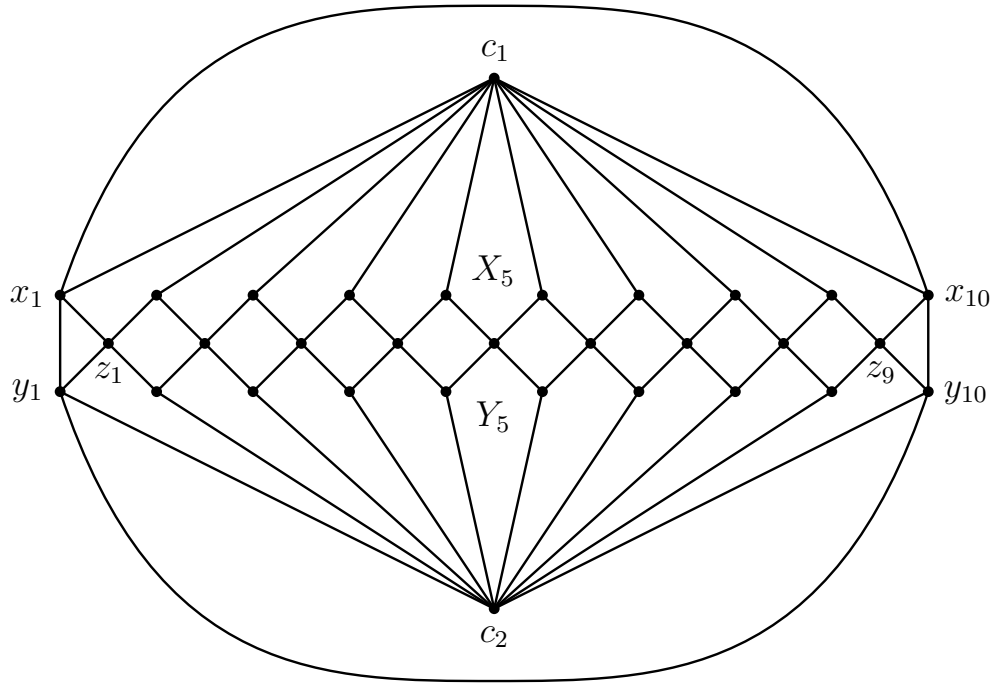

Figure 3.1: The graph H from Construction 3.5. Some vertices and faces are exemplary labeled. Vertices and faces are numbered from left to right.

In the following, we show that it is not always possible to find a 2-clustered planarization edge set, that is, a planarization edge set that is a matching. Furthermore, it follows that we must allow a maximum degree and a maximum path length of at least 2 in our planarization edge sets, improving on the previously mentioned trivial lower bounds for the clustering, defect, and path length of improper 4-colorings.

Construction 3.5:
We begin by constructing a planar graph H, which serves as the planar skeleton of our 1-planar graph. It consists of two instances of the star $K_{1,10}$. Each pair of subsequent edges of the stars has an additional vertex forming a 4-face with them, shared between both stars. Additional edges make all faces of H 3- or 4-faces.

Formally, H is a graph so that:

$$\begin{aligned} V(H) =& \{c_1, c_2\} \cup \{x_i, y_i \mid i \in \{1, ..., 10\}\} \cup \{z_i \mid i \in \{1, ..., 9\}\} \\ E(H) =& \{c_1x_i, c_2y_i \mid i \in \{1, ..., 10\}\} \\ & \cup \{z_ix_i, z_ix_{i+1}, z_iy_i, z_iy_{i+1} \mid i \in \{1, ..., 9\}\} \\ & \cup \{x_1y_1, x_{10}y_{10}, x_1x_{10}, y_1y_{10}\} \end{aligned}$$

Consider the drawing of H shown in Figure 3.1. For $i \in \{1, ..., 9\}$, we define X_i and Y_i as the 4-faces of H bounded by the cycles $c_1, x_i, z_i, x_{i+1}, c_1$ and $c_2, y_i, z_i, y_{i+1}, c_2$, respectively.

We define G as the graph obtained from H by adding a pair of crossing edges into each 4-face of H. By construction, G is TQ-embedded.

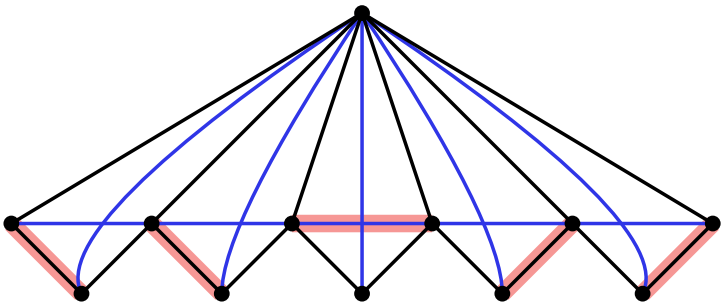

Figure 3.2: If a planarization edge set P is a matching and contains no edges incident to the star's center, P containing a single crossing edge fully determines P for this subgraph of G from Construction 3.5. Edges in P are highlighted in red.

Theorem 3.6: *The graph G from Construction 3.5 admits no planarization edge set that is a matching.*

Proof. Let H be the planar skeleton of G. By Lemma 2.31, a set $P \subseteq E(G)$ is a planarization edge set of G if and only if it hits all 4-faces of H. Assume for the sake of contradiction that there exists a planarization edge set P of G such that P is a matching.

Our goal is to show that for some $i \in \{1, ..., 9\}$, the set P contains multiple edges incident to z_i, contradicting P being a matching. To that end, we show that P hits at least one of the faces X_i and Y_i using an edge not incident to z_i for at most eight $i \in \{1, ..., 9\}$.

As P is a matching, P contains at most one edge incident to c_1 and c_2 each. Each edge hits at most two 4-faces. Thus, P hits at least one of X_i and Y_i using an edge incident to c_1 or c_2 but not to z_i for at most four $i \in \{1, ..., 9\}$.

Now consider the case that there exists a nonempty interval $\{k, ..., l\} \subseteq \{1, ..., 9\}$ such that P does not contain any of the edges in $\{c_1x_k, ..., c_1x_{l+1}, c_1z_k, ..., c_1z_l\}$. In that case, if P contains the edge x_ix_{i+1} for some $i \in \{k, ..., l\}$, then the matching property of P fully determines which edges in P hit the faces $X_k, ..., X_l$ (see Figure 3.2). In particular, P contains the edge x_ix_{i+1} for at most one $i \in \{k, ..., l\}$.

The set P contains at most one edge incident to c_1. Therefore, the set of $i \in \{1, ..., 9\}$ such that P does not hit X_i using an edge incident to c_1 can be partitioned into at most two intervals with the properties described above. Thus, P hits X_i using the edge x_ix_{i+1} for at most two $i \in \{1, ..., 9\}$. Note that x_ix_{i+1} is the only edge hitting X_i that is incident to neither c_1 nor z_i, and no edge hitting X_i is incident to c_2. Therefore, P hits X_i using an edge incident to neither c_1, c_2, nor z_i for at most two $i \in \{1, ..., 9\}$

Analogously, P hits Y_i using an edge incident to neither c_1, c_2, nor z_i for at most two $i \in \{1, ..., 9\}$. ∎

3.1 Reduction to TQ-Embedded Graphs

In this section, we reduce the problem of finding clustered 4-colorings via clustered planarization edge sets from all 1-planar graphs to TQ-embedded graphs. As a coloring of a graph induces a coloring of all its subgraphs, it suffices to consider maximally 1-embedded graphs. In particular, we use maximally 1-embedded graphs that are also well-embedded. As a first step towards our reduction, we show that such an embedding always exists.

Lemma 3.7: *Let $G_0 = (V, E)$ be an embedded 1-planar graph. Then there exists an embedded supergraph $G \supseteq G_0$ that is both maximally 1-embedded and well-embedded.*

Proof. We iteratively construct the graph G. We start with the 1-embedding of G_0.

If the current 1-embedding is not maximal, we add edges so that we obtain a maximal 1-embedding. Then, as long as the current embedding is not a well-embedding, we redraw edges one by one to reduce the number of crossings until we arrive at a well-embedding.

We repeat that process until we arrive at an embedding that is both a maximal 1-embedding and a well-embedding. In each step, we either add an edge or we reduce the number of crossings in the embedding without changing the graph. We do not add new vertices to our graph. Thus, the number of edges is upper-bounded by $4|V| - 8$ according to Proposition 2.20, and the number of crossings is lower-bounded by 0. Therefore, our process finishes after a finite number of steps. ∎

For this section, let G be a maximally 1-embedded well-embedded graph and let H be the planar skeleton of G.

Next, we analyze the structure of the H. First, we remark that H is 2-connected.

Proposition 3.8 (Eades et al., 2013 [Ead+13])**:** *Let $G = (V, E)$ be a maximally 1-embedded graph such that $|V| \geq 3$. Let H be the planar skeleton of G. Then H is 2-connected.*

Note that Proposition 3.8 implies that every face of the planar skeleton H is bounded by a cycle.

To prove our reduction, we need to study the relationship between faces of the planar skeleton H and crossing edge pairs of G found within them. Recall that as G is maximally 1-embedded and well-embedded, the endpoints of a pair of crossing edges in G form a cycle in the planar skeleton by Lemma 2.26. The following lemma is a complementary statement to that fact.

Lemma 3.9: *Let G be a maximally 1-embedded and well-embedded graph. Let H be the planar skeleton of G.*

Let C be a closed Jordan curve in the embedding of G with the following properties:

- *All points of C lie on a vertex or edge of G.*
- *No edge of G crosses C.*
- *At least four vertices lie on C.*
- *The interior $\mathrm{int}(C)$ contains no vertices and no uncrossed edges.*

Then there exists at least one pair of crossing edges within $\mathrm{int}(C)$.

Proof. Let $V(C)$ denote the set of vertices on C and let $n = |V(C)|$. Observe that as no edge of G crosses C, for each crossed edge that $\mathrm{int}(C)$ contains a part of, $\mathrm{int}(C)$ fully contains the interiors of both edges of the corresponding crossing edge pair.

Assume for the sake of contradiction that there is no pair of crossing edges in $\mathrm{int}(C)$. Then $\mathrm{int}(C)$ is a connected component of the plane in the embedding of G. Thus, by maximality of the 1-embedding of G, the vertex set $V(C)$ induces a subgraph isomorphic to K_n in G. Furthermore, because G is well-embedded, all edges of $G[V(C)]$ are uncrossed.

Because $\mathrm{int}(C)$ is a connected component of the plane, it is possible to add a new vertex v to $\mathrm{int}(C)$ so that v is joined to each vertex of $V(C)$ via an uncrossed edge. Thereby, we obtain a planar drawing of K_{n+1}. That is a contradiction, as $n \geq 4$ and K_5 is not planar. ∎

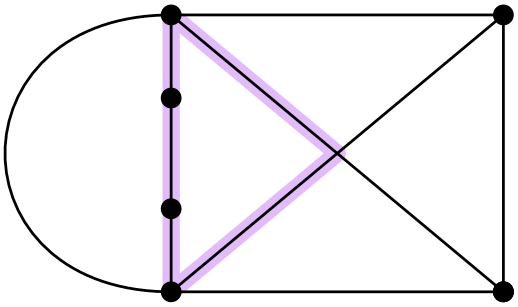

Figure 3.3: Curve fulfilling the criteria from Lemma 3.9. Note that the depicted graph is not maximally 1-embedded and thus, Lemma 3.9 does not apply.

Important examples of the curves described in Lemma 3.9 are the boundaries of faces of the planar skeleton H. Another example of such a curve is depicted in Figure 3.3.

The previous lemmas show that maximal 1-planar well-embeddings are closely related to TQ-embeddings: Every face of H is bounded by a cycle, G contains a crossing edge pair within each k-face of H with $k \geq 4$, and for every crossing edge pair in G, the endpoints of the crossing edges form a 4-cycle in the planar skeleton. Note, however, that the edges of the 4-cycle formed by the endpoints of a crossing edge pair do not necessarily belong to the same face of H as the crossing edge pair itself. These insights lead us to a structure characteristic of maximal 1-planar well-embeddings that are not TQ-embeddings: large face separators.

Definition 3.10 (Large Face Separator)**:** *Let G be a maximally 1-embedded well-embedded graph. Let ac and bd be edges of G crossing at point Z.*

For $\{x, y\} \in \{\{a, b\}, \{b, c\}, \{c, d\}, \{d, a\}\}$, the closed curve C formed by the edge xy and the segments of ac and bd between x, Z, and y, is called a large face separator *if* $\mathrm{int}(C)$ *contains at least one vertex.*

Figure 3.4 shows a large face separator.

Lemma 3.11: *Let $G = (V, E)$ be a maximally 1-embedded well-embedded graph such that $|V| \geq 4$. Let H be the planar skeleton of G. For each k-face f of H with $k \geq 5$, G contains a large face separator intersecting f.*

Proof. Let f be a k-face of H such that $k \geq 5$. By Proposition 3.8, the boundary of f is a cycle. Therefore, by Lemma 3.9, there exists a pair of crossing edges x_1x_3 and x_2x_4 of G within f. The boundary of f contains the vertices x_1, x_2, x_3, x_4 in that cyclic order. As $k \geq 5$, the boundary of f contains a path $v_1, ..., v_l$ with $l \geq 3$ and $(v_1, v_l) = (x_i, x_{i+1})$ for some $i \in \{1, 2, 3, 4\}$, where i is understood modulo 4.

By Lemma 2.26, the edge v_1v_l exists in H. The edge v_1v_l is outside of f. Thus, the interior of the curve C, formed by v_1v_l and the parts of x_1x_3 and x_2x_4 up to the crossing point, contains the vertex v_2. Therefore, C is a large face separator. ∎

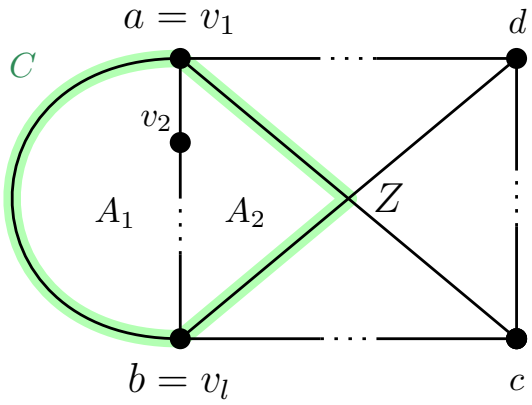

Figure 3.4: Large face separator in a maximally 1-embedded well-embedded graph. Vertices, curves, points, and areas are labeled as named in the proof of Theorem 3.12.

Next, we prove the main Theorem for our reduction.

Theorem 3.12: *If there exist $k, \Delta \in \mathbb{N}_0$ so that all TQ-embedded graphs admit a k-clustered planarization edge set with maximum degree at most Δ, then all maximally 1-embedded well-embedded graphs admit a $(4\Delta + 1)k$-clustered planarization edge set.*

Proof. Assume there exist $k, \Delta \in \mathbb{N}_0$ so that all TQ-embedded graphs admit a k-clustered planarization edge set with maximum degree at most Δ.

Let $G = (V, E)$ be a maximally 1-embedded well-embedded graph. Without loss of generality, let $|V| \geq 4$. Let H be the planar skeleton of G. By Proposition 3.8, every face of H is bounded by a cycle. By Lemma 3.9, every 4-face of H contains a crossing edge pair. Thus, G is TQ-embedded if and only if H does not contain a face of degree at least 5.

We do induction on the number n of large face separators in G.

Induction Base: For $n = 0$, G does not contain a face of degree at least 5 by Lemma 3.11. Therefore, G is TQ-embedded. Thus, G admits a k-clustered planarization edge set by our premise.

Induction Hypothesis: Every maximally 1-embedded well-embedded graph containing at most n large face separators admits a $(4\Delta + 1)k$-clustered planarization edge set.

Induction Step: Let G contain $n+1$ large face separators. Let B be the boundary of the outer face of H. If the crossing points on all large face separators of G lie in $\text{ext}(B)$, we invert $\text{int}(B)$ and $\text{ext}(B)$ by reflecting our drawing of G in B. Note that the resulting drawing is a maximal 1-embedding and a well-embedding, and it has the same crossings as our original drawing.

We choose a large face separator C so that the crossing point Z on C is in $\text{int}(B)$, and $\text{int}(C)$ is inclusion-minimal among all large face separators with their crossing points in $\text{int}(B)$. Let f be the face of H that contains the crossing point Z, and let ac and bd be the corresponding pair of crossing edges. Without loss of generality, a and b are the two vertices on C. Let $v_1, ..., v_l$ be the path on the boundary of f from a to b. Note that $(v_1, v_l) = (a, b)$.

The path $v_1, ..., v_l$ subdivides $\text{int}(C)$ into two areas A_1 and A_2. Let A_2 be the area incident to Z. By Lemma 2.26, the edge ab exists in H. As C is a large face separator, we have $l \geq 3$, and ab is outside of f. See Figure 3.4 for a visualization of the structure of G around C.

Let $G' = G - \text{ext}(C)$, and let H' be the planar skeleton of G'. We claim that G' is TQ-embedded and H' has a 3-face as its outer face.

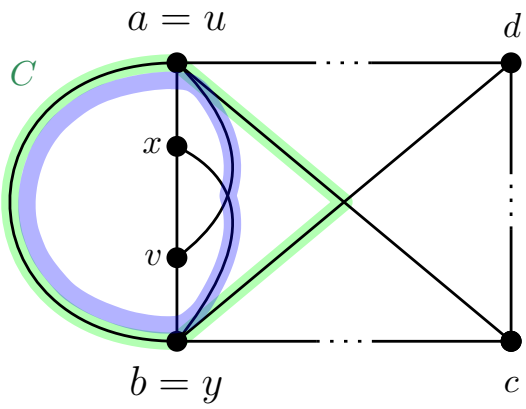

Figure 3.5: If the path $v_1, ..., v_l$ contains more than 3 vertices (here: $l = 4$), we arrive at a contradiction to the inclusion-minimality of $\text{int}(C)$.

Every inner face of H' is a face of H. Thus, every inner face of H' is bounded by a cycle and G' contains a pair of crossing edges within every inner 4-face of H'. By inclusion-minimality of $\text{int}(C)$ and Lemma 3.11, every inner face of H' is a 3-face or 4-face.

The edge ab and the path $v_1, ..., v_l$ form the boundary of the outer face of G'. We claim that $l = 3$ and thus, the outer face of G' is a 3-face.

Assume for the sake of contradiction that $l \geq 4$. As A_2 is a subset of f, A_2 contains no vertices or uncrossed edges. Then by Lemma 3.9 applied to the curve through $v_1, ..., v_l$, ac, and bd bounding A_2, there exists a pair of crossing edges uv and xy within A_2. The vertices u, v, x, and y are distinct vertices on $v_1, ..., v_l$. By Lemma 2.26, the vertices u, x, v, y form a 4-cycle in H. At least one edge e of that 4-cycle is not part of the path $v_1, ..., v_l$. As A_2 does not contain uncrossed edges, e is either equal to ab, or e lies in A_1. In both cases, e, uv, and xy form a large face separator D so that $\text{int}(D) \subsetneq \text{int}(C)$, contradicting the inclusion-minimality of $\text{int}(C)$ (see Figure 3.5).

Thus, G' is TQ-embedded. By our premise, G' admits a k-clustered planarization edge P'_0 set with maximum degree at most Δ.

Recall that as G' is TQ-embedded, an edge set $X \subseteq E(G')$ is a planarization edge set if and only if X hits all 4-faces of H' by Lemma 2.31. For every 4-face f of H', the vertices of f induce a subgraph isomorphic to K_4 in G'. Thus, G' contains an edge hitting f that is incident to neither a nor b.

The set P'_0 contains at most Δ edges incident to a and b each. Together, they hit at most 4Δ 4-faces of H'. We modify P'_0 by replacing all edges incident to a or b with edges neither incident to a nor to b, that hit all 4-faces hit by the replaced edges. The resulting planarization edge set P' contains at most 4Δ edges not present in P'_0, thus each cluster of P' is a subset of the union of at most $4\Delta + 1$ clusters in P'_0. Thus, P' is $(4\Delta + 1)k$-clustered.

Let $G'' = G - \text{int}(C)$. The removal of $\text{int}(C)$ creates no new large face separators and makes C no longer a large face separator. Thus, G'' contains at most n large face separators.

Next, we show that G'' is maximally 1-embedded. Assume for the sake of contradiction that it is possible to add an edge e to the drawing of G''. As G is maximally 1-embedded, the edge e intersects $\text{int}(C)$. The vertices a and b are the only vertices incident to $\text{int}(C)$ in G''. Thus, a or b is an endpoint of e. As ab exists in G'', the other endpoint of e is in $\text{ext}(C)$. Thus, e crosses C.

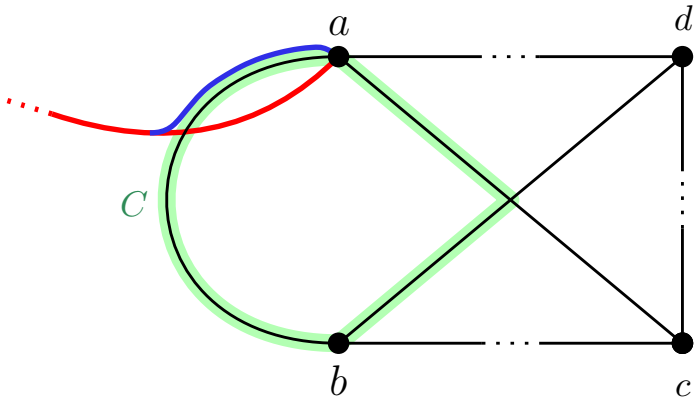

Figure 3.6: If it is possible to draw an edge e in G' crossing ab, it is also possible to draw e in G while avoiding $\text{int}(C)$. Red: drawing of e as added to G', blue: alternative drawing of e possible in G.

Specifically, e crosses the edge ab, as the rest of C consists of vertices and crossed edges. As the edge ab is uncrossed in G'', it is possible to draw e alongside of ab to avoid $\text{int}(C)$ (see Figure 3.6). Therefore, e can also be drawn in G, contradicting the maximality of the embedding of G.

Next, we show that G'' is well-embedded, that is, it is not possible to redraw any crossed edge of G'' as an uncrossed edge. Assume for the sake of contradiction that it is possible to redraw a crossed edge e in G'' as an uncrossed edge. As G is well-embedded, we must redraw e so that e intersects $\text{int}(C)$. If e is neither ac nor bd, then the new drawing of e does not cross C and thus, we redraw e without intersecting $\text{int}(C)$, contradicting the well-embeddedness of G. Thus, e equals ac or bd. Without loss of generality, let $e = ac$. Then a, b, d, and the subpath of the boundary of f between d and a form a cycle D in the planar skeleton of $G'' - e$ (see Figure 3.6). Note that $\text{int}(C) \subseteq \text{int}(D)$. As c lies in $\text{ext}(D)$ and we redraw e as an uncrossed edge, we redraw e without intersecting $\text{int}(C)$, contradicting the well-embeddedness of G.

G'' has at most n large face separators, is maximally 1-embedded, and well-embedded. By our induction hypothesis, G'' admits a $(4\Delta + 1)k$-clustered planarization edge set P''.

The set $P := P' \cup P''$ is a planarization edge set of G. As a and b form a separator and P' contains no edge incident to a or b, every cluster of P is either a cluster of P' or a cluster of P''. Thus, P is $(4\Delta + 1)k$-clustered. ∎

Together with Lemmas 3.4 and 3.7, we obtain the following corollary from Theorem 3.12.

Corollary 3.13: *Let G be a 1-planar graph. If there exist $c, \Delta \in \mathbb{N}$ so that all TQ-embedded graphs admit a c-clustered planarization edge set with maximum degree at most Δ, then G admits a $(4\Delta + 1)c$-clustered 4-coloring.*

4 TQ-Embedded Graphs

In this chapter, we discuss approaches for applying Theorem 3.12 by finding planarization edge sets with bounded clustering for TQ-embedded graphs.

We begin by analyzing structural properties of TQ-embedded graphs. First, we observe that every TQ-embedding is a well-embedding.

Lemma 4.1: *Let $G = (V, E)$ be a TQ-embedded graph. Then G is well-embedded.*

Proof. Let D be the embedding of G, and let H be the planar skeleton of G with respect to D. Let $uv \in E$ be an edge.

Assume for the sake of contradiction that we can redraw uv in D to obtain an embedding of G with fewer crossings than D. Then uv is a crossed edge in D, and it is possible to redraw uv as an uncrossed edge. As D is a TQ-embedding, uv is drawn within a 4-face f of H. As it is possible to redraw uv as an uncrossed edge, u and v have a common incident face f' of H other than f. Because uv, as drawn in D, is not uncrossed, uv does not exist in H. Therefore, f' is a 4-face of H with u and v not adjacent on the boundary of f'. Then, as G is TQ-embedded, G contains the edge uv both in f and in f'. That contradicts G being simple. ∎

For TQ-embedded graphs, we observe that the planar skeleton and the associated planar graph are 3-connected.

Lemma 4.2: *Let $G = (V, E)$ be a TQ-embedded graph such that $|V| \geq 4$, and let H be the planar skeleton of G. Then H is 3-connected.*

Proof. Observe that because every face of H has a cycle as its boundary, H is 2-connected.

Assume for the sake of contradiction that H is not 3-connected. Then there exist vertices $x, y \in V$ such that H' is disconnected, where $H' = H - x - y$. Let H_1 be a connected component of H' and let $H_2 = H' - H_1$. As H is 2-connected, both H_1 and H_2 contain at least one vertex that is adjacent to x in H and at least one vertex that is adjacent to y in H. Thus, x and y have at least two common incident faces f_1 and f_2 in H (see Figure 4.1).

If f_1 is a 3-face, then the boundary of f_1 contains the edge xy. If f_1 is a 4-face, then the edge xy exists either on the boundary of f_1 or as a crossing edge from G within the interior of f_1. Analogously, the boundary or the interior of f_2 contains the edge xy.

Because G is simple, xy lies in the intersection of the boundaries of f_1 and f_2. That contradicts both H_1 and H_2 containing at least one vertex (see Figure 4.1). ∎

Lemma 4.3: *Let $G = (V, E)$ be a TQ-embedded graph such that $|V| \geq 4$, and let G^x be the associated planar graph of G. Then G^x is 3-connected.*

Proof. Let H be the planar skeleton of G. By Lemma 4.2, H is 3-connected. The graph H is a subgraph of G^x that spans all true vertices. Furthermore, all cross-vertices of G^x have four distinct neighbors that all exist in H. Therefore, G^x is 3-connected. ∎

Note that the 3-connectivity implies that every face of H and G^x is bounded by a cycle.

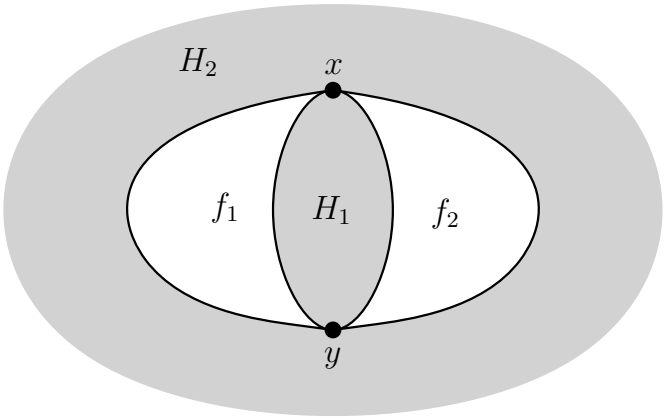

Figure 4.1: The cut vertex pair x and y from the proof of Lemma 4.2 with the two common incident faces. Note that depending on the graph, H_1 and H_2 may be swapped.

4.1 Approach using Triangle Representations

Our first approach for finding planarization edge sets uses the triangle representation of the planar skeleton.

Recall that for a TQ-embedded graph, the planar skeleton is 3-connected according to Lemma 4.2. Therefore, by Proposition 2.36, the planar skeleton of a TQ-embedded graph always admits a triangle representation.

Recall that the contact points of a triangle representation can be classified into six types as depicted in Figure 2.6. Based on that classification, we define a type of edge in the represented graph.

Definition 4.4 (In-Edge)**:** *Let G be a TQ-embedded graph, H the planar skeleton of G, and T a triangle representation of H. We call an edge $e \in E(H)$ an* in-edge *if the contact point representing e in T has the type dual-left, dual-right, or dual-horizontal.*

We use in-edges to find planarization edge sets.

Lemma 4.5: *Let G be a TQ-embedded graph, H its planar skeleton, and T a triangle representation of H. The set P of all in-edges with respect to T is a planarization edge set of G with maximum degree at most 3.*

Proof. As G is TQ-embedded, P is a planarization edge set if and only if P hits all 4-faces of H by Lemma 2.31.

Let f be a 4-face of H, and let d_f be the dual triangle representing f in T. The edges on the boundary of f in H correspond to the contact points on the boundary of d_f in T.

Observe that contact points of the types primal-left, primal-right, or primal-horizontal lie on the corners of both incident dual triangles (see Figure 2.6). As d_f has three corners, at least one contact point on the boundary of d_f has one of the types dual-left, dual-right, or dual-horizontal. The corresponding edge of H on the boundary of f is an in-edge. Thus, P hits f.

Observe that a contact point representing an in-edge is always located at a corner of both incident primal triangles (see Figure 2.6). Thus, the maximum degree of P is at most 3. ∎

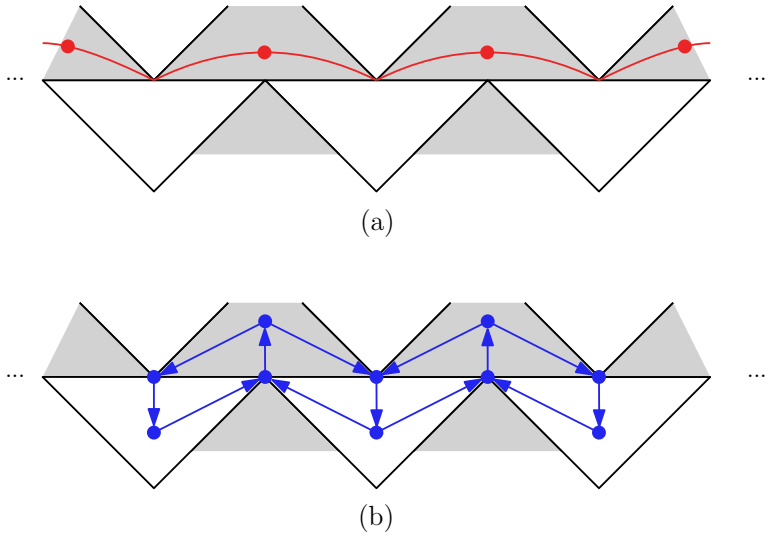

Figure 4.2: Construction for arbitrarily long paths formed by in-edges. (a) depicts the formed path. (b) depicts part of the auxiliary graph of the triangle representation around the formed path.

As the set of all in-edges with respect to any triangle representation has a bounded maximum degree by Lemma 4.5, the only potential problem for clustering is unbounded path length according to Lemma 2.33.

In Figure 4.2, we demonstrate a trivial construction for arbitrarily long paths formed by in-edges. However, that construction is only possible in triangle representations with both clockwise and counterclockwise cycles.

In the following, we demonstrate that we cannot always reverse cycles of a triangle representation so that the set of in-edges in the resulting representation is clustered. We do this by constructing a family of triangle representations without directed cycles for which the set of in-edges forms arbitrarily long paths.

Construction 4.6:
For $l \in \mathbb{N}, l \geq 2$, we construct a triangle representation containing a path of length l formed by in-edges.

We start with two dual triangles d_1 and d_2, connected via a primal-horizontal contact point. The triangle d_2 is positioned to the left of d_1, and the tip of d_2 is lower than the tip of d_1.

For each $i \in \{3, ..., l+2\}$, we do the following: Add a new dual triangle d_i so that the ends of its base touch the tip of d_{i-2} and the side of d_{i-1}. We place the tip of d_i so that the outer side of d_i forms a straight line with the outer side of d_{i-2}. For $i < l+2$, we place the tip of d_i lower than the tip of d_{i-1}. For $i = l+2$, we instead place the tip of d_i at the same height as the tip of d_{i-1}.

Finally, we add three primal triangles to the left, right, and top of the construction to obtain the tiling property of the triangle representation.

Figure 4.3 shows the result of this construction for $l = 5$.

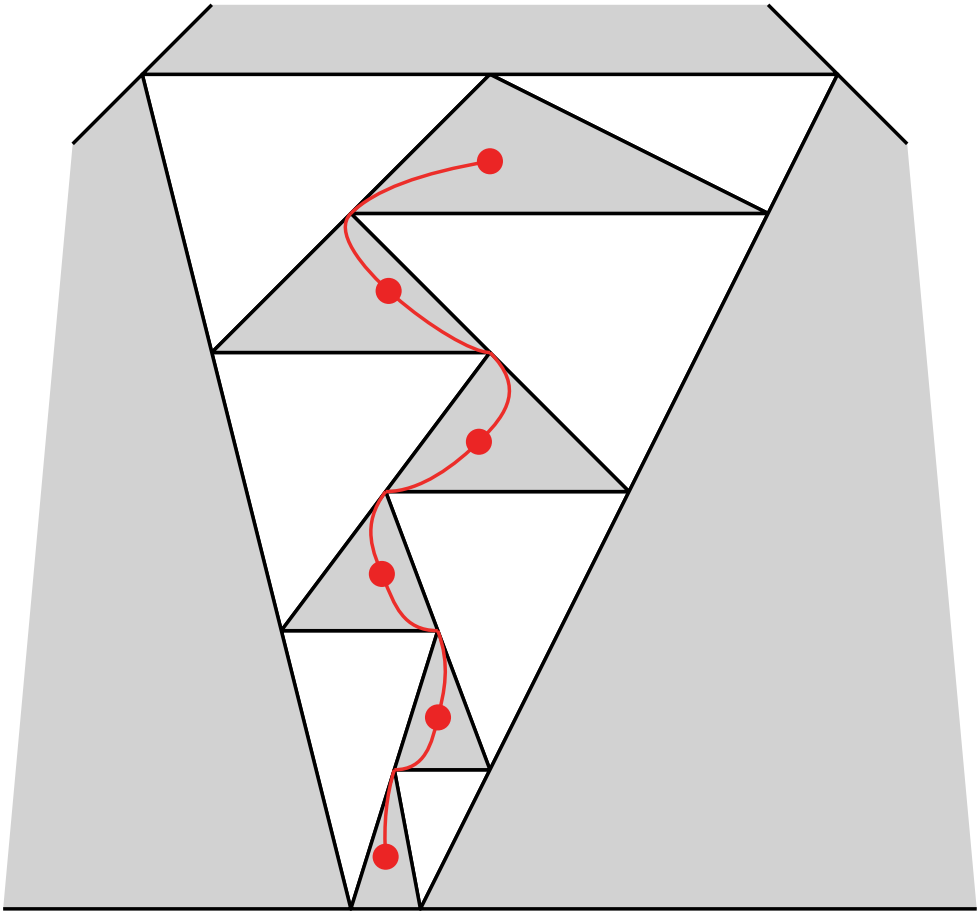

Figure 4.3: The triangle representation from Construction 4.6 for $l = 5$.

Lemma 4.7: *For all $l \in \mathbb{N}, l \geq 2$, the triangle representation from Construction 4.6 contains no directed cycle.*

Proof. Consider the drawing of the auxiliary graph as described in Section 2.5.1.

As the auxiliary graph is bipartite, with the edge-vertices and the triangle-vertices as the bipartition, any directed cycle contains at least two triangle-vertices. We show that no triangle-vertex is on a directed cycle, and thus, no directed cycles exist.

Note that the outgoing edges from all edge-vertices on the boundary of the representation lead to the vertex f_∞ of the auxiliary graph, which is a drain. Thus, none of these edge-vertices is on any directed cycle. The vertices representing the three final primal triangles have outgoing edges only to edge-vertices on the boundary of the representation, and therefore are not on any directed cycle.

All other primal triangle-vertices, as well as the triangle-vertices of d_1 and d_{l+2}, have no ingoing edges (see Figure 4.3) and are thus not on any directed cycle.

For $i \in \{2, ..., l+1\}$, the triangle-vertex of d_i has exactly one ingoing edge, coming from the edge-vertex of its contact point with d_{i+1}. Thus, all directed walks visit these triangle-vertices in strictly decreasing order. Therefore, none of the triangle-vertices d_2, ..., d_{l+1} is on any directed cycle. ∎

In Construction 4.6, most 4-faces have more than one incident in-edge. In particular, picking every other in-edge along the path yields a set of edges that still hits all 4-faces and has bounded clustering. That leads to the question of whether a clustered subset of in-edges that hits all 4-faces always exists. We give a negative answer to this question for triangle representations without counterclockwise cycles.

To construct a counterexample, we analyze the graphs with the following property.

Definition 4.8 ((k, l)-regularity)**:** *Let $G = (V, E)$ be a graph. The graph G is called (k, l)-regular if G is bipartite and there exists a proper 2-coloring $V = R \dot\cup B$ such that $deg(v) = k$ for all $v \in R$ and $deg(v) = l$ for all $v \in B$.*

The property of (k, l)-regularity lets us find a class of graphs for which no proper subset of the in-edges with respect to any triangle representation is a planarization edge set.

Lemma 4.9: *Let G be a TQ-embedded graph, let H be the planar skeleton of G, and let T be a triangle representation of H. If H^* is (3, 4)-regular, then no proper subset of the set of in-edges with respect to T is a planarization edge set of G.*

Proof. Let H^* be (3, 4)-regular. Then in H, each 4-face shares edges only with 3-faces and vice versa. Thus, in T, dual triangles representing 4-faces only touch triangles representing 3-faces and vice versa.

Let S be a proper subset of the in-edges with respect to T. Let e be an in-edge such that $e \notin S$. Consider the dual triangle d whose side the contact point representing e touches. The triangle d represents a 4-face. All corners of d touch triangles representing 3-faces because of the (3, 4)-regularity of H^*. Thus, the edges represented by these corners are not in-edges. Therefore, S does not hit the 4-face represented by d. Thus, S is not a planarization edge set of G by Lemma 2.31. ∎

We give a construction for a family of minimal triangle representations of graphs with a (3, 4)-regular dual for which the set of in-edges forms arbitrarily long paths.

Construction 4.10:
For $l \in \mathbb{N}$ such that $l \equiv 0 \pmod 3$, we construct a triangle representation containing a path of length l formed by in-edges.

In the following, we refer to a dual triangle representing a k-face as a *k-triangle*. We use three building blocks B_1, B_2, and B_3 for our construction, as depicted in Figure 4.4. We use triangle representations without counterclockwise cycles for each building block.

B_1 is a single 3-triangle.

B_2 is a tiled triangle which has a 4-triangle at its left corner and 3-triangles at its other two corners. All contact points representing in-edges of 4-triangles in B_2 are in the interior of B_2. We treat the rest of B_2 as a black box.

B_3 is a tiled triangle which has a 4-triangle d at its right corner and 3-triangles at its other two corners. The contact point representing the in-edge of d lies along the base of B_3. All other contact points representing in-edges lie in the interior of B_3. We treat the rest of B_3 as a black box as well.

In the following, the terms *left corner*, *right corner*, *tip*, and *base* always refer to corners and sides as depicted in Figure 4.4, regardless of the rotation of the specific instance of a building block described in the construction.

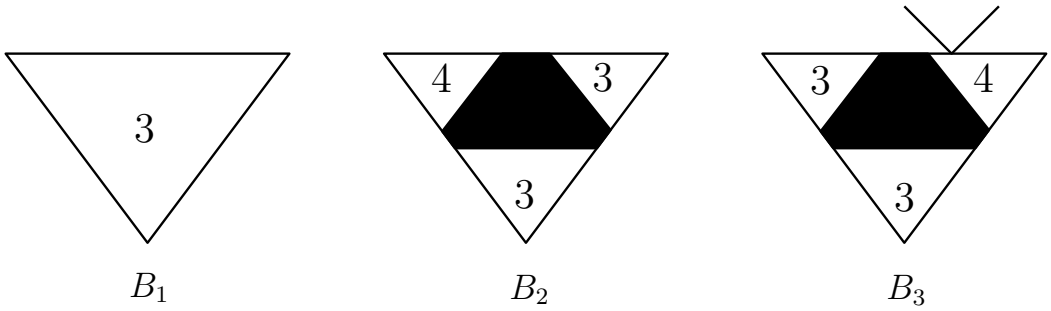

Figure 4.4: The building blocks for Construction 4.10. The numbers indicate the degree of the face represented by the corresponding triangle.

We build a path formed by in-edges in the shape of a spiral.

We begin with one instance of B_1, B_2, and B_3 each, named a_1, a_2, and a_3, respectively. The right corner of a_1 touches the left corner of a_2. The tips of a_1 and a_2 are at the same height. The right corner of a_3 is connected to the tip of a_2. The in-edge of the right 4-face of a_3 belongs to the tip of a_1.

Then, for all $i \in \{4, ..., l + 2\}$, we add an instance of B_3 named a_i. We rotate and scale a_i so that its right corner touches the left corner of a_{i-1}, and the tip of a_{i-3} belongs to the in-edge on the base of a_i.

Finally, we add three primal triangles to the top, left, and right of the construction to obtain the tiling property.

Figure 4.5 shows Construction 4.10 for $l = 3$.

Next, we verify the existence of (3, 4)-regular graphs matching the building blocks B_2 and B_3.

Lemma 4.11: *There exist internally 3-connected planar (3, 4)-regular graphs matching the building blocks B_2 and B_3.*

Proof. Recall that a triangle representation T of a graph tiles a triangle so that the tip of T points upwards and the corners of T belong to primal triangles. The triangle that T tiles represents the outer face of the graph.

On the other hand, the tips of our building blocks point downwards, and the corners belong to dual triangles. Furthermore, they interface with our construction instead of representing an outer face as the tiled triangle.

We resolve these differences by giving suspension graphs with vertices matching the dual triangles of our building blocks. We then rotate the triangle representations of those graphs by 180 degrees to obtain the building blocks.

Recall from Section 2.5.1 that the half-edges of the suspension reaching into the outer face correspond to the corners of the triangle representation. As our building blocks integrate into a larger triangle representation, we need to count the half-edges towards the vertex degrees of our graphs. Analogously, the in-edge on the base of B_3 corresponds to an ingoing half-edge.

Figures 4.6 and 4.7 show such graphs. ∎

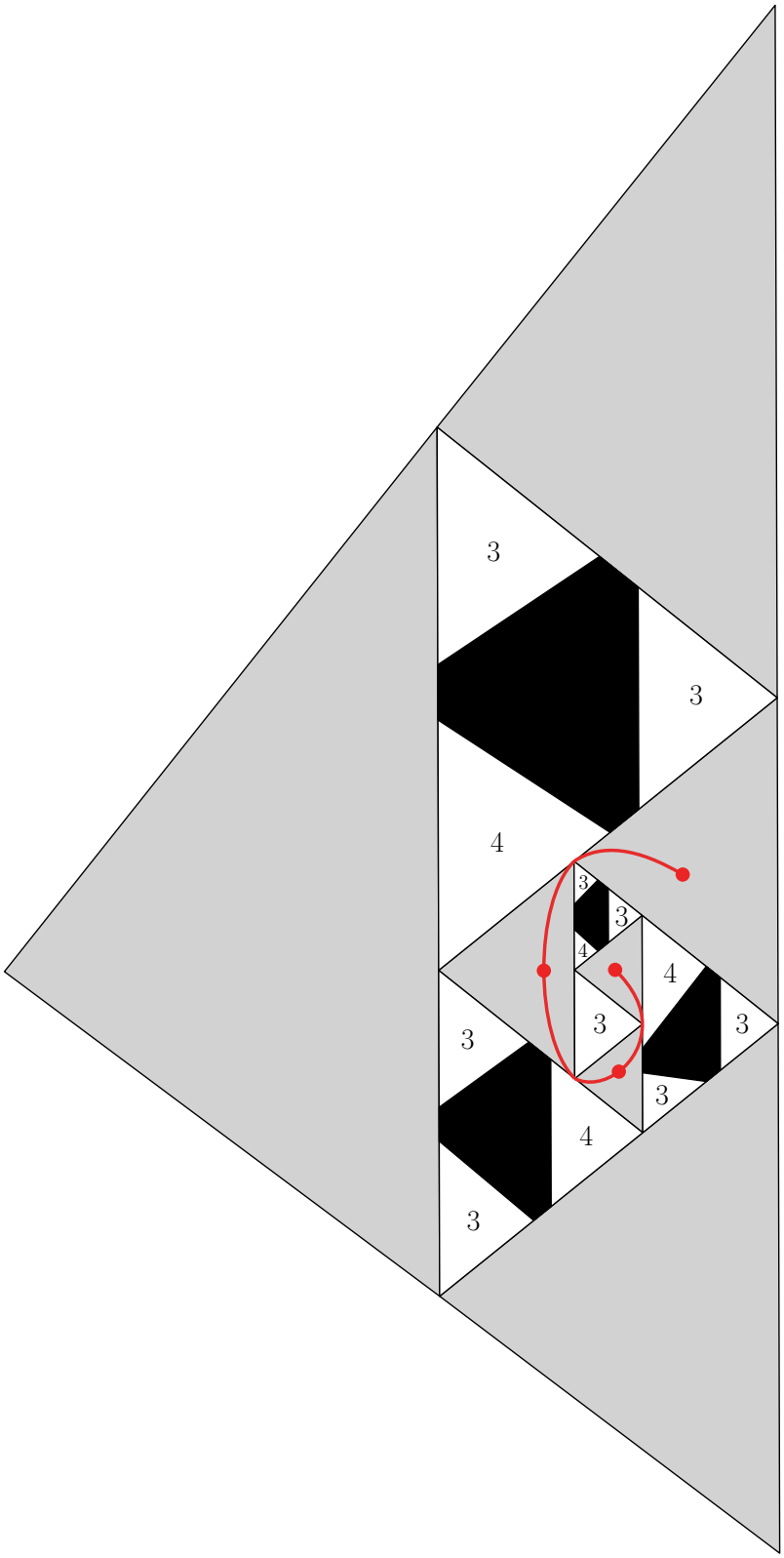

Figure 4.5: Construction 4.10 for $l = 3$. The numbers indicate the degree of the face represented by the corresponding triangle. We depict the construction rotated by 90 degrees.

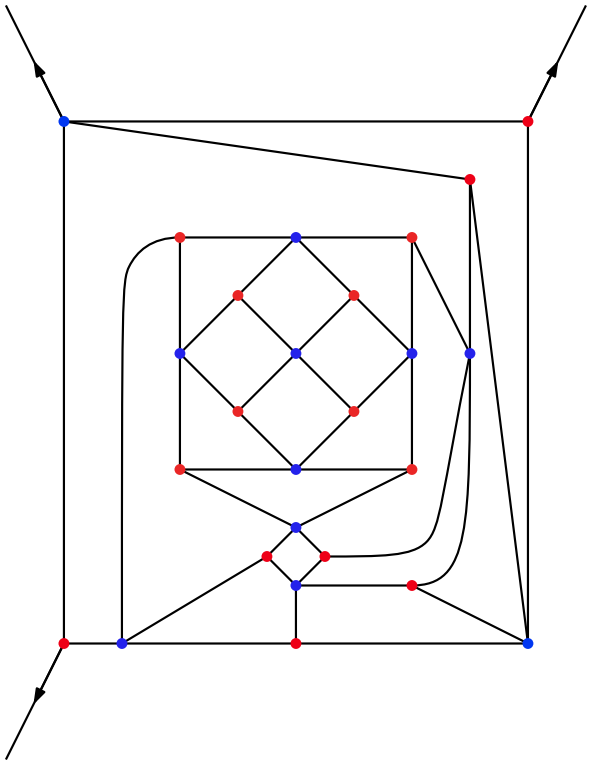

Figure 4.6: Graph matching the building block B_2 from Construction 4.10.

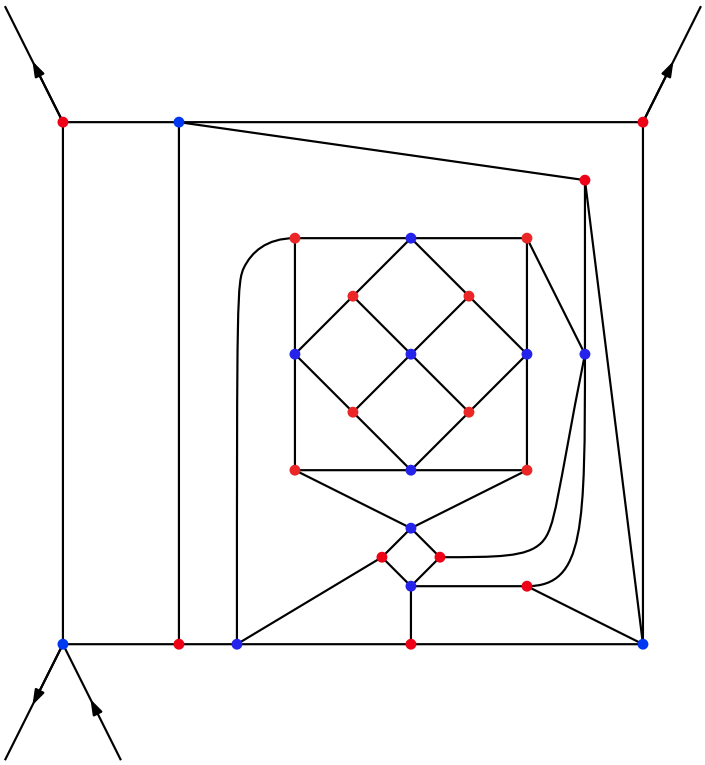

Figure 4.7: Graph matching the building block B_3 from Construction 4.10.

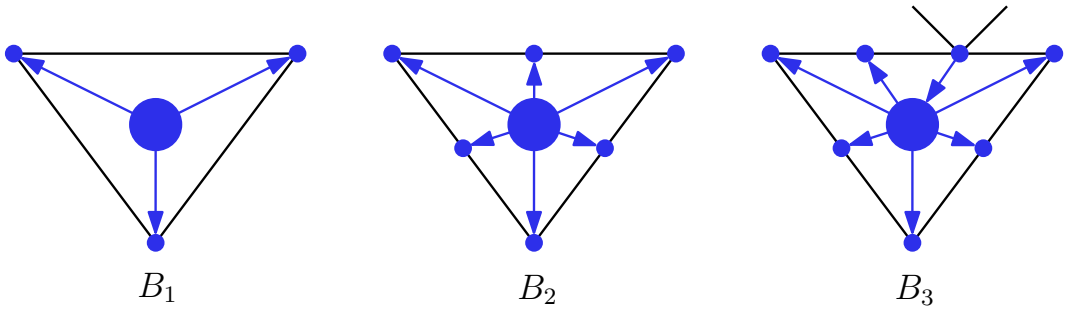

Figure 4.8: The simplified auxiliary graphs of the three building blocks from Lemma 4.12.

Finally, we verify that the triangle representation from Construction 4.10 does not contain counterclockwise cycles.

Lemma 4.12: *For all $l \in \mathbb{N}$ such that $l \equiv 0 \pmod 3$, the triangle representation from Construction 4.10 contains no counterclockwise cycle.*

Proof. By Proposition 2.42, triangle representations of the building blocks B_1, B_2, and B_3 without counterclockwise cycles exist. It remains to show that the interaction of the building blocks in Construction 4.10 does not form any counterclockwise cycle.

To simplify the analysis, we abstract from the auxiliary graph inside of each building block by contracting it to a single vertex, as depicted in Figure 4.8. Furthermore, we deduplicate outward-pointing edge-vertices along the outer sides of the building blocks. That way, for any cycle in the triangle representation, there is a cycle of the same direction in our simplification. We show that our simplified version of the auxiliary graph still contains no counterclockwise cycle.

We use the term *central vertices* to refer to the vertices representing the interior of a building block, as well as the vertices representing a single triangle.

As the simplified auxiliary graph is bipartite, with the edge-vertices and the central vertices as the bipartition, any directed cycle contains at least two central vertices.

First, we observe that the central vertices of B_1 and B_2 have only outgoing edges. The same holds for the central vertices of the final three primal triangles. Thus, none of these central vertices is on any directed cycle.

Next, we define a vertex ordering σ on the central vertices of the primal triangles and the instances of B_3. To do that, we walk along the path formed by in-edges, starting at the innermost primal triangle. Each time we encounter a primal triangle, we append its central vertex at the end of σ. Each time we encounter an in-edge, we consider the 4-triangle d incident to the in-edge. We append to σ the central vertex of the B_3-instance to which d belongs.

We then append the central vertex of the left, top, and right final primal triangle in that order to σ. Finally, we append the vertex representing the outer face to σ. Observe that σ contains $2l + 5$ vertices. The first vertex of σ is $\sigma(1)$. Furthermore, except for the last four vertices, the central vertices of primal triangles and of instances of B_3 alternate in σ.

Let $i \in \{1, ..., 2l + 4\}$. We observe the following property of our ordering: Consider the central vertex $\sigma(i)$ and its neighborhood $N(\sigma(i))$ of edge-vertices. For $e \in N(\sigma(i))$, let $c(e)$ be the central vertex to which e has an outgoing edge.

If $\sigma(i)$ belongs to an instance of B_3, then for all $e \in N(\sigma(i))$ we have $\sigma^{-1}(c(e)) > i$.

If $\sigma(i)$ belongs to a primal triangle, then for all $e \in N(\sigma(i))$ we have $\sigma^{-1}(c(e)) \geq i - 1$.

From that, it follows that all directed cycles in our triangle representation have the form $[\sigma(i)$ - edge vertex - $\sigma(i+1)$ - edge vertex - $\sigma(i)]$, where $\sigma(i)$ is an instance of B_3. We observe that these cycles are all clockwise.

We provide a visualization of the simplified auxiliary graph for $l = 3$ in Figure 4.9. ■

Lemma 4.9 and Construction 4.10 show that a clustered subset of in-edges hitting all 4-faces does not exist for all minimal triangle representations. This leads us to discard the approach of constructing planarization edge sets based on in-edges.

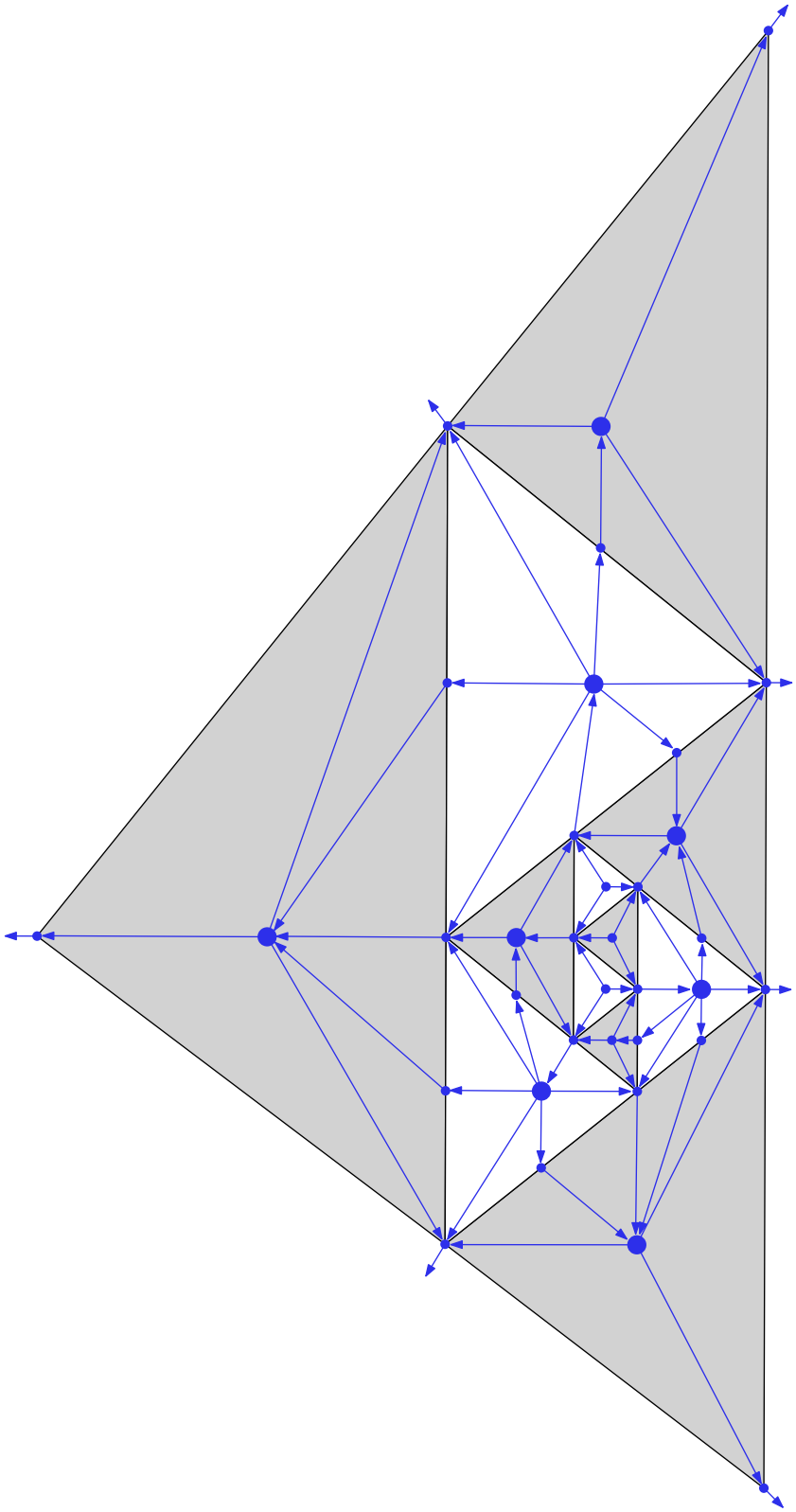

Figure 4.9: The simplified auxiliary graph of the triangle representation from Construction 4.10 for $l = 3$. We depict the construction rotated by 90 degrees.

4.2 Reduction to Rectangular Duals

In this section, we reduce the problem of finding clustered planarization edge sets from all TQ-embedded graphs to those for which the associated planar graph admits a rectangular dual. As an intermediate step, we reduce the problem of finding clustered planarization edge sets from all TQ-embedded graphs to those for which the planar skeleton contains no separating triangles in Theorem 4.14.

Recall that by Lemma 4.2, the planar skeleton of a TQ-embedded graph on at least four vertices is 3-connected. The following lemma shows an important property of separating triangles in 3-connected planar graphs.

Lemma 4.13: *Let G be a 3-connected embedded planar graph and let T be a triangle in G. Then T is a separating triangle if and only if T is not the boundary of a face of G.*

Proof. Let T be a triangle in G such that T is not the boundary of a face of G. Then both $\text{int}(T)$ and $\text{ext}(T)$ contain at least one edge or vertex. As T is a clique, both $\text{int}(T)$ and $\text{ext}(T)$ contain at least one vertex. As G is planar, T separates the vertices in $\text{int}(T)$ from those in $\text{ext}(T)$.

Now let T be a separating triangle. We show that both $\text{int}(T)$ and $\text{ext}(T)$ contain at least one vertex. Thus, T is not the boundary of a face of G.

Let G_1 and G_2 be distinct connected components of $G - T$. Without loss of generality, G_1 is contained in $\text{ext}(T)$. As G is 3-connected, G_1 and G_2 are both joined to each vertex of T by at least one edge in G. In G, contract all edges within G_1 to obtain a vertex v_{G_1}. The vertex v_{G_1} and the vertices of T induce a planar subgraph isomorphic to K_4. The component G_2 is fully contained in one face of that induced K_4. The only face of the induced K_4 that is incident to all three vertices of T is $\text{int}(T)$. Thus, G_2 is contained in $\text{int}(T)$. Refer to Figure 4.10 for a visualization. ∎

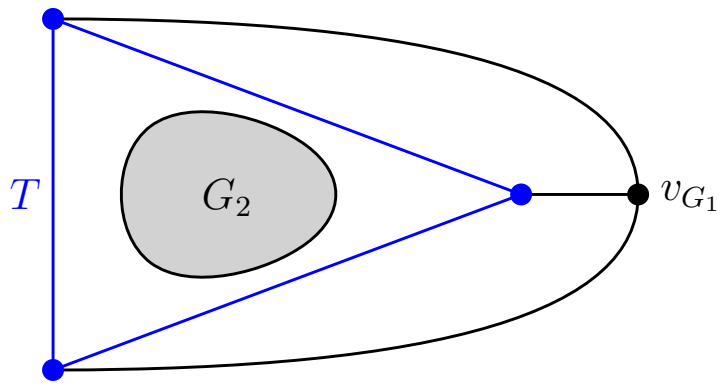

Figure 4.10: The graph obtained from contraction in the proof of Lemma 4.13.

Using Lemma 4.13, we reduce the problem of finding clustered planarization edge sets for TQ-embedded graphs to those for which the planar skeleton contains no separating triangles.

Theorem 4.14: *Let $\mathcal{G}$ be the class of TQ-embedded graphs for which the planar skeleton contains no separating triangle. If there exist $c, \Delta \in \mathbb{N}$ so that all $G \in \mathcal{G}$ admit a c-clustered planarization edge set with maximum degree at most Δ, then all TQ-embedded graphs admit a $(6\Delta + 1)c$-clustered planarization edge set.*

Proof. Assume there exist $c, \Delta \in \mathbb{N}$ so that all $G \in \mathcal{G}$ admit a c-clustered planarization edge set with maximum degree at most Δ.

Let $G = (V, E)$ be a TQ-embedded graph. Without loss of generality, let $|V| \geq 4$. Let H be the planar skeleton of G. Recall that H is 3-connected by Lemma 4.2. We do induction on the number n of separating triangles in H.

Induction Base: For $n = 0$, G admits a c-clustered planarization edge set by our premise.

Induction Hypothesis: All TQ-embedded graphs for which the planar skeleton contains at most n separating triangles admit a $(6\Delta + 1)c$-clustered planarization edge set.

Induction Step: Let H have $n + 1$ separating triangles. We choose a separating triangle T such that $\text{int}(T)$ is inclusion-minimal. Let a, b, and c be the vertices of T. Let $G' = G - \text{ext}(T)$, and let H' be the planar skeleton of G'. Note that G' is TQ-embedded and contains at least four vertices. By Lemma 4.2, H' is 3-connected.

By the inclusion-minimality of T and Lemma 4.13 applied to H, every triangle in H' is the boundary of a face. Notably, T is the boundary of the outer face of H'. As H' is 3-connected, H' contains no separating triangle by Lemma 4.13.

By our premise, G' admits a c-clustered planarization edge P'_0 set with maximum degree at most Δ.

Recall that by Lemma 2.31, an edge set $X \subseteq E(G')$ is a planarization edge set of G' if and only if X hits all 4-faces of H'. We claim that for every 4-face f of H', G' contains an edge hitting f that is not incident to any vertex of T.

As G' is TQ-embedded, the vertices of f induce a subgraph isomorphic to K_4 in G'. Thus, if f contains at most two vertices from T, then our claim holds. Assume for the sake of contradiction that f contains all three vertices of T. Let x be the fourth vertex of f. Without loss of generality, the order of the vertices on the boundary of f is a, b, x, c. Then b, c is a cut vertex pair of H' (see Figure 4.11), contradicting the 3-connectivity of H'.

The set P'_0 contains at most Δ edges incident to a, b, and c each. Together, they hit at most 6Δ 4-faces of H'. We modify P'_0 by replacing all edges incident to vertices of T with edges not incident to any vertex of T, that hit all 4-faces hit by the replaced edges. The resulting planarization edge set P' contains at most 6Δ edges not present in P'_0, thus each cluster of P' is a subset of the union of at most $6\Delta + 1$ clusters in P'_0. Thus, P' is $(6\Delta + 1)c$-clustered.

Let $G'' = G - \text{int}(T)$, and let H'' be the planar skeleton of G''. Analogous to G', the removal of $\text{int}(T)$ from G creates no new separating triangles. By Lemma 4.13, T is not a separating triangle in H''. Thus, H'' contains at most n separating triangles. By our induction hypothesis, G'' admits a $(6\Delta + 1)c$-clustered planarization edge set P''. The set $P := P' \cup P''$ is a planarization edge set of G. As T is a separator and P' contains no edge incident to T, every cluster of P is either a cluster of P' or a cluster of P''. Thus, P is $(6\Delta + 1)c$-clustered. ∎

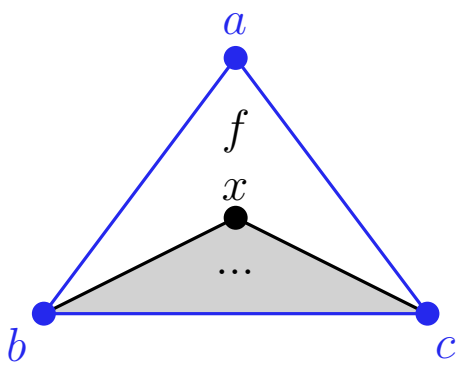

Figure 4.11: In the proof of Theorem 4.14, if a 4-face in H' contains three vertices from the separating triangle T, then a cut vertex pair in H' exists.

The associated planar graphs of the 1-planar graphs in $\mathcal{G}$ from Theorem 4.14 are closely related to planar graphs admitting a rectangular dual. Recall that by Proposition 2.44, for an embedded planar graph G to admit a rectangular dual, it is necessary that all inner faces of G are 3-faces and G contains no separating triangle. Both of these properties apply to the associated planar graphs of TQ-embedded graphs without separating triangles in the planar skeleton.

Lemma 4.15: *Let G be a TQ-embedded graph. Then all faces of the associated planar graph G^x of G are 3-faces.*

Proof. Consider the planar skeleton H of G. The graph H contains only 3- and 4-faces. The 3-faces of H are also 3-faces in G^x. For each 4-face of H bounded by a cycle a, b, c, d, a, there exists a pair of crossing edges ac, bd in G. Let z be the cross-vertex of G^x corresponding to the crossing ac, bd. Then z forms four 3-faces with the vertices a, b, c, and d in G^x. ∎

Lemma 4.16: *Let $G = (V, E)$ be a TQ-embedded graph such that $|V| \geq 4$, H the planar skeleton of G, and G^x the associated planar graph of G. The graph H contains a separating triangle if and only if the graph G^x contains a separating triangle.*

Proof. Recall that by Lemmas 4.2 and 4.3, H and G^x are 3-connected.

Let T be a separating triangle in H. By Lemma 4.13, there exist vertices in both $\text{int}(T)$ and $\text{ext}(T)$. As H is a subgraph of G^x and G^x is planar, T is also a separating triangle in G^x.

Let T be a separating triangle of G^x. We first show that no vertex of T is a cross-vertex and thus T exists in H. Then, we show that T is not the boundary of a face of H and thus, a separating triangle of H by Lemma 4.13.

As G is 1-planar, no two cross-vertices of G^x are adjacent. The triangle T is a clique. Thus, at most one vertex of T is a cross-vertex. As G is TQ-embedded, all triangles of G^x with a cross-vertex are the boundary of a 3-face of G^x and thus, not separating triangles by Lemma 4.13. Therefore, no vertex of T is a cross-vertex.

Now, assume for the sake of contradiction that T is the boundary of a face in H, without loss of generality, an inner face. The graph G contains no edges or vertices in $\text{int}(T)$. Thus, $\text{int}(T)$ contains no cross-vertex in G^x. Thus, T is the boundary of a face in G^x. By Lemma 4.13, that contradicts the 3-connectivity of G^x. ∎

Next, we show that if we remove a single edge from the associated planar graph G^x of a graph $G \in \mathcal{G}$, the resulting graph admits a rectangular dual.

Lemma 4.17: *Let G be a TQ-embedded graph such that $|V(G)| \geq 4$ and the planar skeleton of G contains no separating triangle. Let G^x be the associated planar graph of G, and let e be an edge on the boundary of the outer face of G^x. Then $G^x - e$ admits a rectangular dual.*

Proof. By Lemma 4.15, G^x is a planar triangulation. The deletion of e merges the outer face of G^x with an inner face, both of which are 3-faces. Thus, the outer face of $G^x - e$ is a 4-face, and all inner faces of $G^x - e$ are 3-faces.

Let the cycle a, b, c, a be the boundary of the outer face of G^x and, without loss of generality, $e = bc$. By Lemma 4.16, G^x contains no separating triangle. Assume for the sake of contradiction that $G^x - bc$ contains a separating triangle T.

The inner face of G^x incident to the edge bc is a triangle U. Let b, c, and d be the vertices of U. If $d = a$, then $G^x \cong K_3$, which contradicts $|V(G)| \geq 4$. The separating triangle T contains both a and d, as otherwise all paths from $G^x - T$ could be modified to avoid the edge bc, contradicting T being a separating triangle in $G^x - bc$. Therefore, $ad \in E(G^x - bc)$.

Thus, G^x contains the three triangles $\{a, b, d\}$, $\{a, c, d\}$, and $\{b, c, d\}$. By Lemma 4.13, these three triangles are faces of G^x. In particular, there is no vertex in the interior of any of these triangles. Furthermore, a, b, and c form the boundary of the outer face of G^x. Therefore, G^x is isomorphic to K_4, contradicting the existence of a separating triangle in $G^x - bc$.

The outer face of $G^x - e$ is a 4-face, all inner faces of $G^x - e$ are 3-faces, and $G^x - e$ contains no separating triangle. By Proposition 2.44, $G^x - e$ admits a rectangular dual. ∎

In Section 4.3, we discuss approaches for finding clustered planarization edge sets of TQ-embedded graphs for which the planar skeleton contains no separating triangles. These approaches are based on the rectangular dual of the associated planar graphs.

Another way to use the structural insight on the associated planar graph is in conjunction with a theorem by Whitney.

Proposition 4.18 (Whitney, 1931 [Whi31])**:** *Every planar triangulation without separating triangles admits a Hamilton cycle.*

Lemma 4.19: *Let $G = (V, E)$ be a TQ-embedded graph such that $|V| \geq 4$ and the planar skeleton of G contains no separating triangle. Then G admits a planarization edge set with maximum degree 2.*

Proof. Consider the associated planar graph G^x. By Lemmas 4.15 and 4.16, G^x is a triangulation without separating triangles. By Proposition 4.18, G^x admits a Hamilton cycle C. We construct a Hamilton cycle C' in G so that the edges of C' form a planarization edge set of G.

Let ac, bd be a pair of crossing edges in G, and let z be the corresponding cross-vertex in G^x. The cycle C visits z exactly once. If C contains the edges az and zc, we replace az and zc with ac in C'. Analogously, if C contains the edges bz and zd, we replace them with bd in C'. Otherwise, the predecessor x and the successor y of z on C are adjacent in G, and we replace xz, zy with xy in C'.

Refer to Figure 4.12 for a visualization of the construction of C' from C. ∎

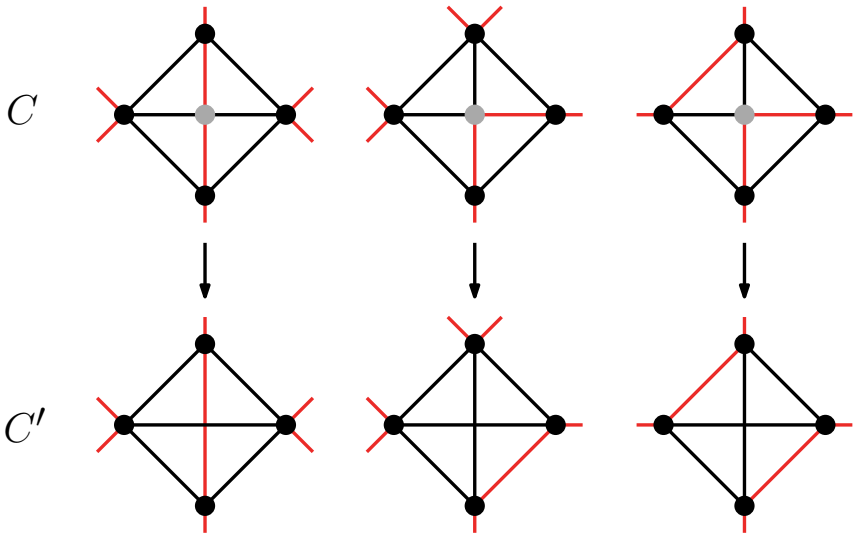

Figure 4.12: Construction of the Hamilton cycle C' in Lemma 4.19.

While the maximum degree of the planarization edge set from Lemma 4.19 is 2, it forms a single cluster containing all vertices of G. As the number of vertices in a TQ-embedded graph without separating triangles in the planar skeleton is unbounded, the planarization edge set does not have bounded clustering. Furthermore, the maximum vertex degree in such a graph is unbounded as well, thus we obtain the following corollary on defective colorings from Lemma 4.19.

Corollary 4.20: *Let G be a well-embedded 1-planar graph. Let P be a planarization edge set of G with maximum degree d. The 4-coloring of G obtained from the construction in Lemma 3.4 is not necessarily d-defective.*

4.3 Approaches using Rectangular Duals

We focus on approaches for finding planarization edge sets in two special variants of rectangular duals: pierceable rectangular duals and modified rectangular duals.

Let $G = (V, E)$ be a TQ-embedded graph such that the planar skeleton of G contains no separating triangle. Let G^x be the associated planar graph of G, e an edge on the boundary of the outer face of G^x, and $G_D = G^x - e$. By Lemma 4.17, G_D admits a rectangular dual D. We investigate approaches for finding a planarization edge set of G based on D.

A set $P \subseteq E$ is a planarization edge set of G if and only if for every cross-vertex z of G_D, the set P contains an edge hitting the crossing corresponding to z.

Consider a cross-vertex z of G_D and the rectangle R_z representing z in D. If z is not an endpoint of e, then $\deg(z) = 4$. Therefore, no meeting point of three rectangles lies along the interior of any side of R_z. Thus, D represents the uncrossed edges of G hitting the crossing of z as rectangle side segments starting at the corners of R_z. Furthermore, D represents the crossing edges of G corresponding to z as a pair of opposing sides of R_z. Figure 4.13 visualizes the relationship between R_z and the edges of G hitting the crossing corresponding to z.

As G is simple, no two rectangles representing cross-vertices share both the top and the bottom neighbors. Analogously, no two rectangles representing cross-vertices share both the left and right neighbors.

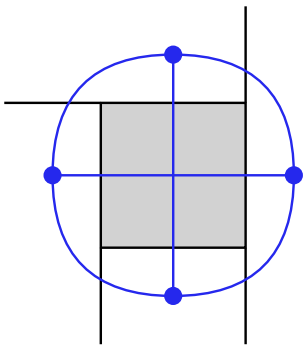

Figure 4.13: Rectangle representing a cross-vertex z in the rectangular dual of G_D. The corresponding vertices of G and the edges hitting the crossing corresponding to z are drawn in.

Recall that by Proposition 4.18, G^x admits a Hamilton cycle and thus, a Hamilton path. If G_D admits a pierceable rectangular dual, we obtain a Hamilton path with stronger properties regarding the order in which it visits the neighbors of cross-vertices.

Lemma 4.21: *Let G be a TQ-embedded graph such that the planar skeleton of G contains no separating triangle. Let G^x be the associated planar graph of G, and let e be an edge on the boundary of the outer face of G^x.*

If $G^x - e$ admits a pierceable rectangular dual, then there exists a directed Hamilton path P in $G^x - e$ such that:

For every cross-vertex z of G^x, if z is not an endpoint of e, then exactly two neighbors b and l of z are predecessors of z on P. Let t and r be the other two neighbors of z. The edges bl and tr exist in $G^x - e$.

We call b and l preceding neighbors *of z, and we call t and r* succeeding neighbors *of z.*

Proof. Let $G^x - e$ admit a pierceable rectangular dual D. Walking along the piercing diagonal from the bottom-left corner of D to the top-right corner of D yields a directed Hamilton path P of G^x by definition of pierceablility.

Let z be a cross-vertex of G^x such that z is not an endpoint of e, and let R_z be the rectangle representing z in D. Let b, l, t, and r be the vertices represented by the rectangle to the bottom, left, top, and right of R_z, respectively. The piercing diagonal enters R_z from the left or bottom side and exits R_z from the right or top side. Thus, b and l are predecessors of z on P while t and r are successors of z on P.

The rectangles representing b and l meet at the bottom-left corner of R_z, thus $bl \in E(G^x - e)$. Analogously, the rectangles representing t and r meet at the top-right corner of R_z, thus $tr \in E(G^x - e)$. ∎

As G is TQ-embedded, the neighbors of a cross-vertex in G^x form a 4-cycle in G^x. An idea for using the Hamilton path P from Lemma 4.21 to construct a planarization edge set is the following.

For each cross-vertex z such that z is not an endpoint of e, choose the edge that joins the two preceding neighbors of z. Another variation of that idea is to choose the edge that joins the direct successor of z on P to a preceding neighbor of z. Note that which preceding neighbor of z is adjacent to the direct successor of z depends on z and D. Therefore, we cannot choose a fixed preceding neighbor in the second variation. As illustrated in Figures 4.14 and 4.15, neither of these approaches yields a planarization edge set with bounded path length.

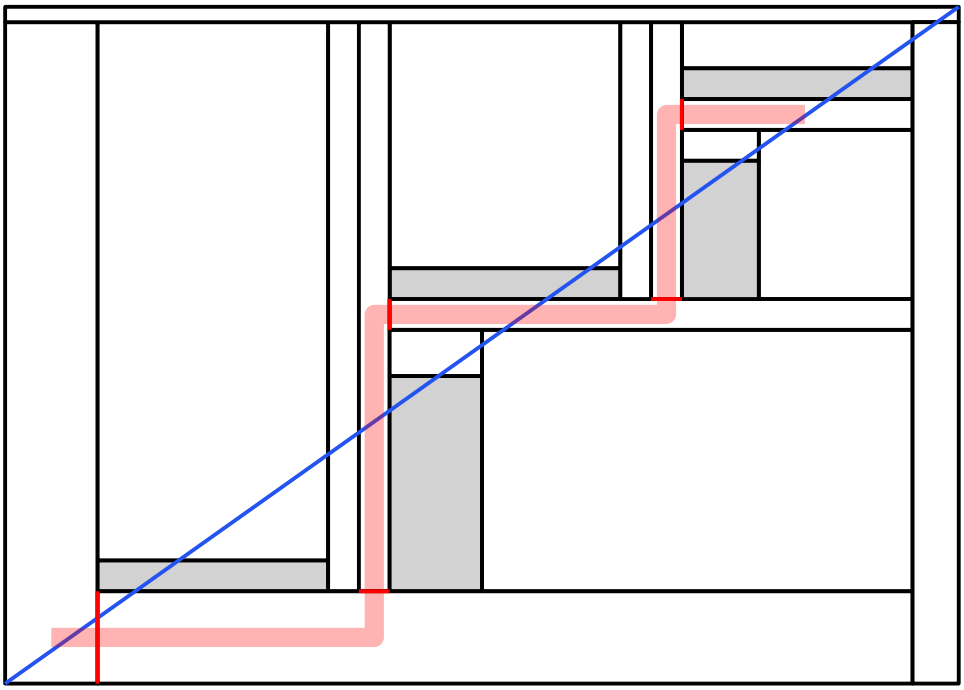

Figure 4.14: Sketch for the construction of an arbitrarily long path formed by the set of edges connecting the two predecessors of each cross-vertex on the Hamilton path from Lemma 4.21.
Gray: cross-vertices, blue: piercing diagonal, red: picked edges, pink: formed path.

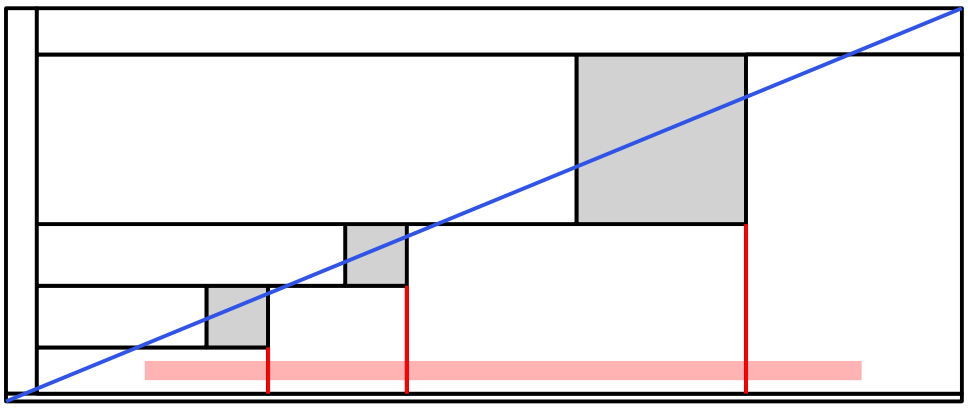

Figure 4.15: Sketch for the construction of an arbitrarily long path formed by the set of edges connecting the direct successor of each cross-vertex on the Hamilton path from Lemma 4.21 to the adjacent predecessor of the cross-vertex.
Gray: cross-vertices, blue: piercing diagonal, red: picked edges, pink: formed path.

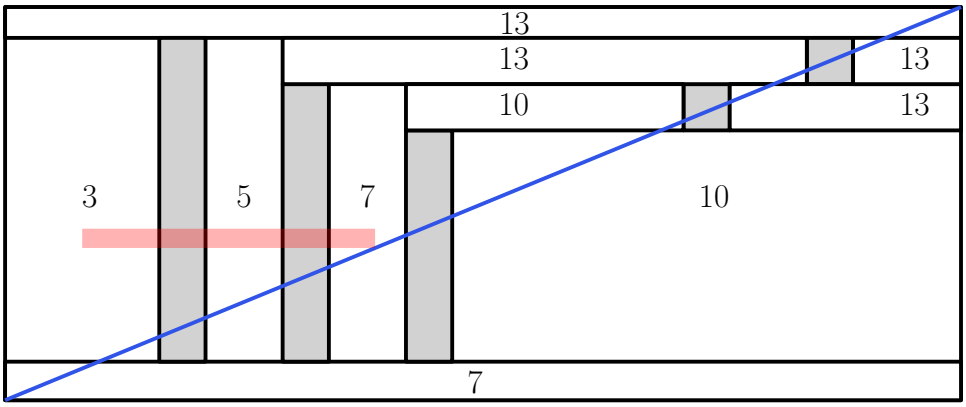

Figure 4.16: Sketch for the construction of an arbitrarily long path formed by the set of edges picked based on the late-value. Rectangles representing true vertices are labeled with their corresponding late-value. When picking only uncrossed edges, the vertex represented by the bottom rectangle has an unbounded number of incident picked edges.
Gray: cross-vertices, blue: piercing diagonal, pink: formed path.

Rotating Figure 4.14 by 180 degrees also covers the variant of choosing the edge that joins the two succeeding neighbors of z. Analogously, Figure 4.15 also covers the variant of choosing the edge that joins the direct predecessor of z on P to a succeeding neighbor of z. Thereby, we cover all variants of choosing uncrossed edges based on the positions of their endpoints on P.

A more global approach to using the vertex ordering induced by the Hamilton path P from Lemma 4.21 is the following.

For $v \in V(G^x)$, let $\sigma(v)$ denote the position of v on P. For $v \in V(G^x)$, we define $\text{late}(v) = \max(\{0\} \cup \{\sigma(u) \mid u \in N(v), u \text{ is cross-vertex}\})$. For $uv \in E$, we define $\text{late}(uv) = \max\{\text{late}(u), \text{late}(v)\}$.

The concept of late-values is inspired by the idea of iterating over the vertices of G^x in the order given by P and choosing edges so that the last iteration impacted by each choice lies as close in the future as possible. To achieve that, for each cross-vertex z of G^x, we pick the edge $e \in E$ hitting the crossing corresponding to z with the minimum $\text{late}(e)$.

However, as illustrated in Figure 4.16, doing so does not yield a bounded path length for our planarization edge set. The path in Figure 4.16 consists of crossing edges of G. If we limit ourselves to uncrossed edges of G, the planarization edge set constructed for Figure 4.16 has an unbounded maximum degree instead.

4.3.1 Modified Rectangular Duals

None of the approaches for constructing planarization edge sets we described so far achieve bounded path length, while some of them achieve bounded maximum degree. To improve our understanding of how to avoid unbounded path length, we investigate a class of 1-planar graphs for which achieving bounded maximum degree is trivial, allowing us to focus on path length. For that, we define a modified variant of rectangular duals in which we drop the requirements that no four rectangles meet at a single point and that exactly four rectangles are on the boundary of the representation. We then analyze TQ-embedded graphs for which the planar skeleton admits a modified rectangular dual. For two special cases, we give constructions for planarization edge sets with bounded clustering.

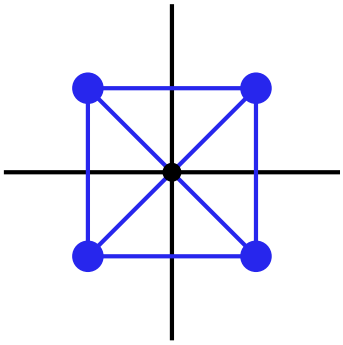

Figure 4.17: Meeting point representing a 4-face f of the planar skeleton in the modified rectangular dual. Black: modified rectangular dual, blue: edges of the 1-planar graph corresponding to f.

Definition 4.22 (Modified Rectangular Dual)**:** *Let G be an embedded 3-connected planar graph. The* modified rectangular dual *represents each vertex of G as a rectangle. Together, all rectangles representing vertices tile a single, larger rectangle. Like the regular rectangular dual, the modified rectangular dual represents each edge of G as a side contact of the rectangles corresponding to the edges' endpoints.*

For each face f of G, the rectangles representing the vertices on the boundary of f meet in a single point. If f is a k-face, we call the corresponding meeting point a k-point.

Note that if an embedded planar graph G admits a modified rectangular dual, each face of G has degree at most 4 and every vertex of G is incident to at most four 4-faces.

Let G be a TQ-embedded graph with a planar skeleton H such that H admits a modified rectangular dual D. Each 4-face f of H corresponds to a 4-point p in D. The rectangle side segments incident to p correspond to the edges on the boundary of f. Furthermore, the crossing edges of G within f correspond to the pairs of rectangles meeting at p diagonally. Refer to Figure 4.17 for a visualization of the relationship between 4-faces of H and 4-points in D.

If H admits a modified rectangular dual, finding a planarization edge set of G with bounded maximum degree is trivial: Picking all segments incident to at least one 4-point yields a planarization edge set with a maximum degree of at most 8. Thus, the only difficulty in finding planarization edge sets for such graphs lies in avoiding paths of arbitrary length.

A simple special case of modified rectangular duals are regular grids of squares. If D is a regular grid of squares, we find a 2-clustered planarization edge set of G by picking every other horizontal segment of each row, with an offset of one space between subsequent rows, as depicted in Figure 4.19.

Next, we consider a generalization of regular grids of squares.

Definition 4.23 (Domino-Covered Grid)**:** *Let D be a modified rectangular dual. If D is obtained from a regular grid of squares by fusing pairs of horizontally adjacent squares, then D is called a* domino-covered grid.

Figure 4.18 shows an example of a domino-covered grid.

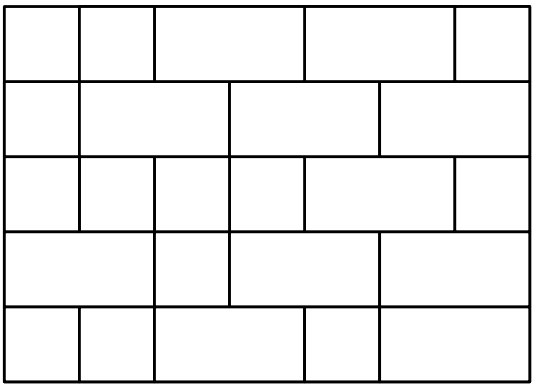

Figure 4.18: Example of a domino-covered grid.

If D is a domino-covered grid, we iteratively construct a clustered planarization edge set.

Theorem 4.24: *Let G be a TQ-embedded graph with a planar skeleton H that admits a representation as a domino-covered grid D. Then G admits an 8-clustered planarization edge set.*

Proof. We denote the i-th row of rectangles and their vertical sides in D as R_i, starting at the bottom of D. For vertical segments s and t within the same row, we define the *distance* between s and t in D as the number of squares between them in the regular grid of squares from which D is obtained. For 4-points p and q, we define $\text{dist}(p, q)$ as the distance between the vertical segments below them.

For any set X of segments of D, we denote the set of edges of G corresponding to the segments in X as E_X. We construct a set of segments P iteratively, row by row, bottom-up, so that E_P is a planarization edge set of G. We only pick vertical segments, thus every cluster of E_P is a path confined to a single row of D.

We call a vertical segment s within R_i a *forced segment* if the lower endpoint of s is a 4-point p, and P does not contain a segment from R_{i-1} incident to p. We maintain as an invariant that after processing R_i, the forced segments of R_{i+1} have a distance of at least 3. Note that R_1 does not have any forced segments, as there are no 4-points along the bottom of D.

We call a pair of 4-points (p, q) on the same horizontal line, with p to the left of q, a *problematic pair* if neither p nor q has an incident segment in P and $\text{dist}(p, q) \leq 2$. We call a triple of 4-points (p, q, r) a *problematic triple* if (p, q) and (q, r) are problematic pairs. For a problematic triple (p, q, r), we define $R(p, q, r)$ as the set of rectangles between the vertical segments below p and r.

For all R_i, we perform the following steps. First, we add all forced segments of R_i to P. Thus, P hits all 4-points in D up to the bottom of R_i. As the left and right segment of each rectangle in D have a distance of at most 2, our invariant ensures that the paths formed by $E_{P \cap R_i}$ contain at most two vertices each.

Second, we eliminate the problematic triples at the top of R_i one by one. In each iteration, we choose a problematic triple (p, q, r) such that $R(p, q, r)$ is inclusion-maximal among all remaining problematic triples. We eliminate the problematic triple by adding all vertical segments between rectangles in $R(p, q, r)$ to P, as depicted in Figure 4.20. As $\text{dist}(p, r) \leq 4$, the path formed by the edges of G corresponding to the picked vertical segments contains at most four vertices.

We show that the segments below p and r remain unpicked, separating the paths created in step 2 from each other. Furthermore, these segments remaining unpicked ensures that each path created in step 1 is either fully contained in a single path created in step 2, or disjoint from all paths created in step 2. Therefore, after the second step, each path formed by $E_{P \cap R_i}$ contains at most four vertices.

Assume for the sake of contradiction that we pick a segment below p or r in a later iteration of step 2, without loss of generality, a segment below r. Then r lies between the endpoints of a problematic triple (x, y, z). In particular, z lies to the right of r. Furthermore, as we pick an incident segment for all 4-points between p and r when we eliminate (p, q, r), either $x = p$ or x lies to the left of p. Thus, $R(p, q, r) \subsetneq R(x, y, z)$, contradicting our choice of problematic triple.

Third, we eliminate all problematic pairs at the top of R_i. For each problematic pair (p, q), we add the vertical segment below p to P. As we eliminate all problematic triples before this step, q is not part of another problematic pair. Thus, we merge groups of at most two paths from step 2, yielding a maximum of eight vertices per path.

By eliminating all problematic triples and pairs, we maintain our invariant. ∎

Note that the planar skeleton from Construction 3.5 does not admit a modified rectangular dual. Thus, we investigate an iterative approach for constructing a matching as a planarization edge set based on modified rectangular duals.

Let G be a TQ-embedded graph such that the planar skeleton H of G admits a modified rectangular dual D. For each 4-point p of D, we assign a fixed priority to each of the six edges of G hitting p, based on the position of the representation of the edges in D. Then we iterate over the 4-points, and for each 4-point p, we pick the edge with the highest priority among all edges hitting p for which neither endpoint has a picked incident edge yet.

For the iteration order of the 4-points, we first choose an ordering σ_R of the rectangles. We direct the edges of H based on D so that each edge corresponding to a vertical segment is directed from the left to the right rectangle and each edge corresponding to a horizontal segment is directed from the bottom to the top rectangle. Then we choose a topological ordering as σ_R. We order the 4-points based on the order in which the rectangles to the top-right of each 4-point appear in σ_R.

Figure 4.21 shows counterexamples for two families of priority assignments. In Figure 4.21a, we assign the highest priority to the segment to the right of each 4-point. All other priorities remain undetermined. Then the 4-point at the bottom-left corner of rectangle 11 has no available edge to pick.

In Figure 4.21b, we assign the highest priority to the segment to the left of each 4-point. All other priorities remain undetermined. The 4-point at the bottom-left corner of rectangle 16 has only the top segment available to pick. Then, the 4-point at the bottom-left corner of rectangle 17 has no available edge to pick.

The fact that both of the aforementioned families of priority assignments only encompass a single decision and still admit counterexamples leads us to discard this approach for finding matchings as planarization edge sets.

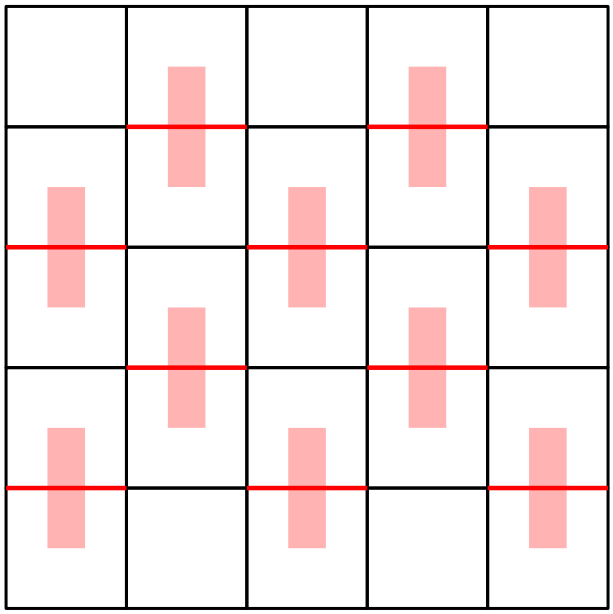

Figure 4.19: Sketch for the construction of a 2-clustered planarization edge set in a modified rectangular dual that is a regular grid of squares. Red: picked edges, pink: formed clusters

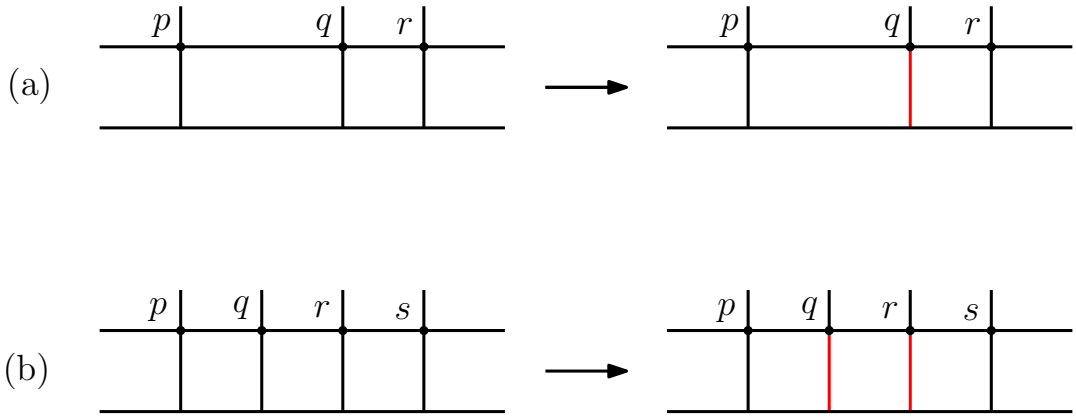

Figure 4.20: Elimination of problematic triples in the proof of Theorem 4.24.
(a) The problematic triple (p, q, r) is eliminated.
(b) There are four problematic triples: (p, q, r), (q, r, s), (p, q, r), and (p, r, s). As we eliminate inclusion-maximal problematic triples, we choose either (p, q, s) or (p, r, s) to eliminate. Here, both choices lead to the same picked edges.

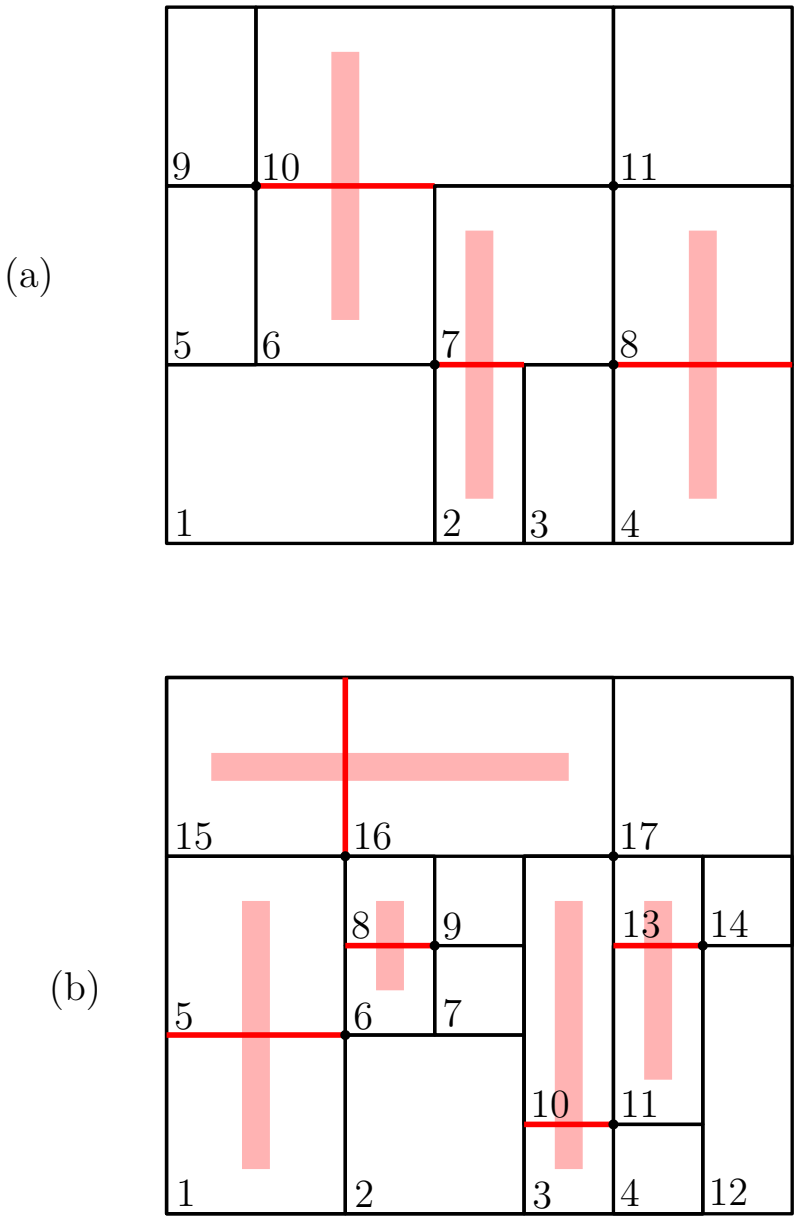

Figure 4.21: Counterexamples for the priority list approach. The numbers signify the rectangle ordering σ_R. The ordering is chosen so that whenever multiple choices for the next rectangle produce a valid topological ordering, we choose the rectangle with the lowest base. Red: picked edges, pink: formed clusters
(a) We assign the highest priority to the segment to the right of each 4-point.
(b) We assign the highest priority to the segment to the left of each 4-point.

5 Optimal 1-Planar Graphs

Although optimal 1-planar graphs contain the maximum number of edges possible for 1-planar graphs, achieving this maximum enforces strong constraints on the structure of the graphs. An important one is the following property of the planar skeleton.

Proposition 5.1 (Czap and Hudák, 2013 [CH13])**:** *Let G be an embedded optimal 1-planar graph, and let Q be its planar skeleton. The planar skeleton Q is a quadrangulation, that is, the boundary of every face of Q is a 4-cycle. Furthermore, for each 4-face f of Q, the graph G contains a pair of crossing edges within f.*

Thus, all embedded optimal 1-planar graphs are TQ-embedded. Using this property, we can show the following theorem.

Theorem 5.2 (Ueckerdt [Uec])**:** *Let G be an embedded optimal 1-planar graph and let Q be its planar skeleton. If Q contains no separating 4-cycle, then G admits a 10-clustered 4-coloring.*

In Section 5.1, we present a proof of Theorem 5.2 based on a proof sketch by Ueckerdt [Uec]. In Section 5.2, we discuss an issue for generalizing Theorem 5.2 to all optimal 1-planar graphs analogously to Theorem 4.14.

5.1 Proof of Theorem 5.2

Let $G = (V, E)$ be an embedded optimal 1-planar graph such that its planar skeleton Q contains no separating 4-cycle. By Proposition 5.1, Q is a quadrangulation.

We first analyze the structure of G and Q to obtain a pair of planar induced subgraphs of G that are dual to each other and cover the vertices of G. That pair of planar graphs allows us to interpret the triangle contact representation from Proposition 2.36 as a representation of Q. Using this representation, we show that G has a 10-clustered planarization edge set.

First, we show that Q is bipartite. To do this, we first show that Q contains no cycle of odd length. Then we show that all graphs without cycles of odd length are bipartite.

Lemma 5.3: *Let Q be a planar quadrangulation. Then Q contains no cycle of odd length.*

Proof. Consider any planar drawing of Q. Assume for the sake of contradiction that Q contains an odd cycle. Let $C^{(0)} = v_0, ..., v_k$ be an odd cycle in Q such that the interior of $C^{(0)}$ is inclusion-minimal among all odd cycles in Q. Note that $v_0 = v_k$.

As $C^{(0)}$ is odd and every face in Q is bounded by a cycle of length 4, the interior of $C^{(0)}$ is not a face. Thus, there exists a path subdividing the interior of $C^{(0)}$. In particular, there exists a subdividing path $P = p_0, ..., p_l$, where $p_0 = v_i$ and $p_l = v_j$ for distinct $i, j \in \{0, ..., k-1\}$ and $\{p_1, ..., p_{l-1}\} \cap \{v_0, ..., v_k\} = \emptyset$. Without loss of generality, $i < j$ holds.

Together with $C^{(0)}$, P forms two cycles $C^{(1)} = v_0, ..., v_i, p_1, ..., p_l, v_{j+1}, ..., v_k$ and $C^{(2)} = v_i, ..., v_j, p_{l-1}, ..., p_0$ (see Figure 5.1).

Observe that $||C^{(1)}|| + ||C^{(2)}|| = ||C^{(0)}|| + 2 \cdot ||P||$. As $||C^{(0)}||$ is odd, $||C^{(1)}|| + ||C^{(2)}||$ is also odd and thus, exactly one of $||C^{(1)}||$ and $||C^{(2)}||$ is odd. The interiors of $C^{(1)}$ and $C^{(2)}$ each are proper subsets of the interior of $C^{(0)}$, contradicting the minimality of the interior of $C^{(0)}$ among all odd cycles. ∎

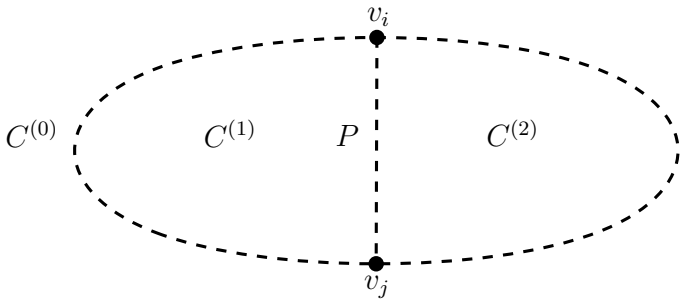

Figure 5.1: The cycle $C^{(0)}$ and the path P form cycles $C^{(1)}$ and $C^{(2)}$

Lemma 5.4: *Let $G = (V, E)$ be a graph with no odd cycle. Then G is bipartite.*

Proof. We present a proof sourced from [MS25].

Let $v \in V$ be any vertex. We consider the 2-coloring $V_1 = \{u \in V \mid \text{dist}(u, v) \text{ is even}\}$ and $V_2 = \{u \in V \mid \text{dist}(u, v) \text{ is odd}\}$. We claim that this 2-coloring is proper.

Assume for the sake of contradiction an edge $ab \in E$ exists so that $\text{dist}(a, v) \equiv \text{dist}(b, v) \mod 2$. Consider a shortest path P_a from v to a and a shortest path P_b from v to b. Let c be the last common vertex of P_a and P_b. Let P'_a and P'_b be the subpaths of P_a and P_b starting from c, respectively. Note that $||P'_a|| + ||P'_b||$ is even. Thus, P'_a and P'_b form an odd cycle together with the edge ab.

∎

By Lemmas 5.3 and 5.4, Q is bipartite. Let R (red) and B (blue) be the color classes of a proper 2-coloring of Q. We define $G_R = G[R]$ and $G_B = G[B]$. Note that G_R, G_B, and Q partition the edges of G. In the following, we call the edges of Q black edges, the edges of G_R red edges, and the edges of G_B blue edges.

We consider the drawings of G_R and G_B obtained from the 1-planar drawing of G by omitting vertices and edges not present in the respective subgraph. As each pair of crossing edges in G consists of one red and one blue edge, these drawings of G_R and G_B are planar.

To interpret a primal-dual triangle representation of G_B as a representation of Q, we show that G_B and G_R are dual to each other. Then, we show that G_B is 3-connected and thus admits a triangle representation as described in Proposition 2.36. To prove these statements, we first show that G_B is 2-connected as an intermediate step.

Lemma 5.5: *Let $G = (V, E)$ be an optimal 1-planar graph, Q its planar skeleton, R and B the color classes of a proper 2-coloring of Q, and $G_B = G[B]$.*

Then G_B is 2-connected.

Proof. Recall that G is TQ-embedded and thus, by Lemma 4.2, Q is 3-connected. Let $c \in B$ be a blue vertex. We show that $G_B - c$ is connected. Let $u, v \in B \setminus \{c\}$.

As Q is 3-connected, $Q - c$ is connected. Thus, there exists a path $P = v_1 \dots v_n, v_1 = u, v_n = v$ connecting u and v in Q. Red and blue vertices alternate on P. We show that for all red vertices v_i on P, there exist two paths $P_i^{(1)}$ and $P_i^{(2)}$ from v_{i-1} to v_{i+1} in G_B such that $P_i^{(1)} \cap P_i^{(2)} = \{v_{i-1}, v_{i+1}\}$. Thus, at least one of $P_i^{(1)}$ and $P_i^{(2)}$ exists in $G_B - c$. Applying that result to all red vertices on P yields a path connecting u and v in $G_B - c$.

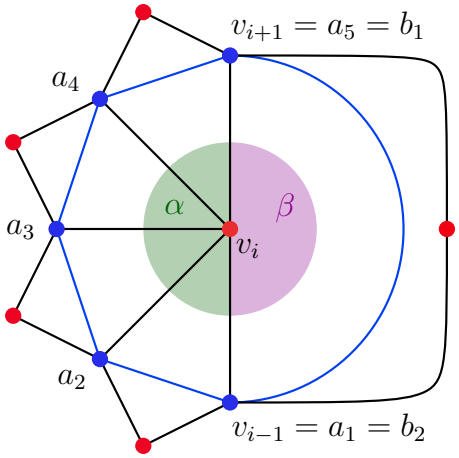

Figure 5.2: A red vertex v_i with the surrounding angles and neighbors as described in the proof of Lemma 5.5. Red edges omitted for clarity.

Let v_i be a red vertex on P. Note that v_i is not an endpoint of P. Consider the two angles α, β between the edges $v_{i-1}v_i$ and v_iv_{i+1}, including these edges themselves. Let $a_1, ..., a_k$ and $b_1, ..., b_l$, in clockwise order, be the blue neighbors of v_i in Q that connect to v_i via an edge in α and β, respectively. Then $\{a_1, ..., a_k\} \cap \{b_1, ..., b_l\} = \{v_{i-1}, v_{i+1}\}$. Refer to Figure 5.2 for a visualization.

For all $j \in \{1, ..., k-1\}$, the edges a_jv_i and $a_{j+1}v_i$ connect to subsequent neighbors of v_i in clockwise order. Thus, the two edges share an incident face in Q. By Proposition 5.1, a_ja_{j+1} exists in G and thus, in G_B. Therefore, $a_1...a_k$ is a path between v_{i-1} and v_{i+1} in G_B. Analogously, $b_1...b_l$ is a path between v_{i-1} and v_{i+1} in G_B.

■

Note that it follows from Lemma 5.5 that the boundary of each face of G_R and G_B is a cycle.

Now, we prove the duality of G_B and G_R.

Lemma 5.6: *Let G be an optimal 1-planar graph, Q its planar skeleton, R and B the color classes of a proper 2-coloring of Q, and $G_B = G[B], G_R = G[R]$.*

Then G_R is dual to G_B, that is, $G_R = G_B^*$.

Proof. We show that our drawing of G_R matches the standard drawing of G_B^* as described in Lemma 2.14.

Let $n = |V(G)|, n_R = |R|, n_B = |B|$ and $m_B = |E(G_B)|$. Let f_B be the number of faces of G_B. Note that $n = n_R + n_B$, and by Proposition 2.25, we have $m_B = n - 2$.

Consider a face f of G_B. Each edge on the boundary of f is crossed by exactly one red edge. As we started with a 1-planar drawing of G, none of these red edges cross a blue edge again. Thus, each of these red edges has an endpoint within the interior of f.

It only remains to show that the interior of f does not contain multiple red vertices. As no red vertex is contained in multiple faces of G_B, and each face contains at least one red vertex, this is equivalent to showing that $n_R = f_B$.

The graph G_B is planar and, by Lemma 5.5, connected, thus we can apply Euler's formula to G_B and obtain:

$$\begin{aligned} & n_B - m_B + f_B = 2 \\ \iff & n_B + n_R - n_R - m_B + f_B = 2 \\ \iff & n - n_R - (n-2) + f_B = 2 \\ \iff & -n_R + f_B = 0 \\ \iff & n_R = f_B \end{aligned}$$

■

In addition to the duality of G_B and G_R, we need the following relationship between G_B, G_R, and the edges of Q.

Lemma 5.7: *Let $G = (V, E)$ be an optimal 1-planar graph, Q its planar skeleton, R and B the color classes of a proper 2-coloring of Q, and $G_B = G[B], G_R = G[R]$.*

By Lemma 5.6, $G_R = G_B^*$.

For all $v \in R$, the blue neighbors of v are exactly the vertices on the boundary of the face v^* corresponding to v in G_B.

Proof. As all edges in G connecting v to blue vertices are black, and black edges are uncrossed, all blue neighbors of v lie on the boundary of v^*.

Let x be any vertex on the boundary of v^*. The vertex x has a neighbor y on the boundary of v^*, that is, the blue edge xy exists and is part of the boundary of v^*. Let $vu = (xy)^*$. The edges vu and xy are a pair of crossing edges in G. As G is optimal, G is maximally 1-embedded, and as G is TQ-embedded, by Lemma 4.1, G is well-embedded. Therefore, by Lemma 2.26, vx exists in Q. ■

Now we can get back to proving that G_B is 3-connected. Recall that Q contains no separating 4-cycle.

Lemma 5.8: *Let $G = (V, E)$ be an optimal 1-planar graph, Q its planar skeleton, R and B the color classes of a proper 2-coloring of Q, and $G_B = G[B]$.*

If Q contains no separating 4-cycle, then G_B is 3-connected.

Proof. We show the contraposition: If G_B is not 3-connected, then Q contains a separating 4-cycle.

Let G_B not be 3-connected. Then there exists a pair of vertices $x, y \in B$ such that G'_B is disconnected, where $G'_B = G_B - x - y$. Let G_1 be a connected component of G'_B and let $G_2 = G'_B - G_1$. By Lemma 5.5, G_B is 2-connected. Thus, both G_1 and G_2 contain at least one vertex that is adjacent to x in G_B and at least one vertex that is adjacent to y in G_B. As G_B contains no edges between G_1 and G_2, it follows that x and y share two distinct incident faces in G_B.

By Lemmas 5.6 and 5.7, we find a red vertex adjacent to both x and y in each of these faces. Together with x and y, they form a separating 4-cycle in Q as depicted in Figure 5.3.

■

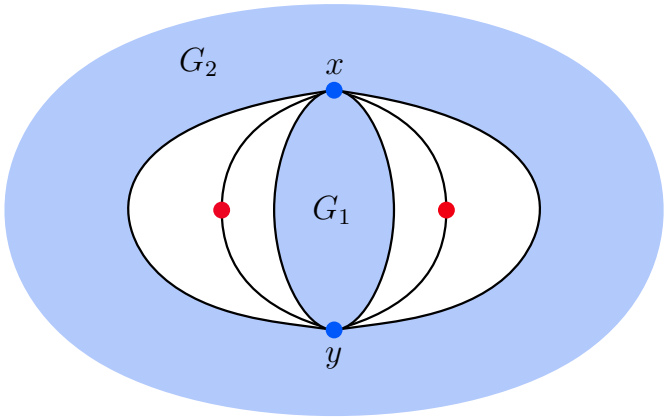

Figure 5.3: The subgraphs G_1 and G_2 of G_B from the proof of Lemma 5.8, together with the faces of G_B enclosed by the boundaries of $G_B - G_1$ and $G_B - G_2$.

Consider a minimal triangle representation T of G_B. Recall that a minimal triangle representation contains no counterclockwise cycles in the corresponding s-orientation.

Each contact point of T corresponds to an edge of G_B and its dual edge. By Lemma 5.6, this is equivalent to a pair of crossing edges from G. The contact points divide each side of each triangle of T into segments. We observe that because of Lemma 5.7, each segment of T corresponds to a black edge of G and vice versa.

These properties let us interpret T as a representation of Q: Each 4-face of Q corresponds to a contact point of T with the incident segments corresponding to the edges of the 4-face.

Recall that we classify contact points of T into six types as depicted in Figure 2.6. For our representation T, this classification also applies to the 4-faces of Q.

Now, we find a planarization edge set using T:

Construction 5.9 (Ueckerdt [Uec])**:**
Let $G = (V, E)$ be an optimal 1-planar graph, Q its planar skeleton, B a color class of a proper 2-coloring of Q, and $G_B = G[B]$. Let T be a minimal triangle representation of G_B.

We construct an edge set $P \subseteq E$ by picking the corresponding segments in T using the following set of rules:

For each primal triangle t of T:

(R1) If the 4-faces at both ends of the base of t are horizontal and no primal triangle's tip touches the base of t, pick no segments of t.

(R2) If (R1) does not apply to t, pick the leftmost and rightmost segment along the base of t.

(R3) Let $t_1, ..., t_k$ be the primal triangles whose tips touch the interior of the base of t, ordered from left to right based on the position of their tips. If $k \geq 3$, pick the uppermost segment on the left side of $t_2, ..., t_{k-1}$.

For each dual triangle d of T, we define a rule symmetric to (R3):

(R4) Let $d_1, ..., d_k$ be the dual triangles whose tips touch the interior of the base of d, ordered from left to right based on the position of their tips. If $k \geq 3$, pick the lowermost segment on the right side of $d_2, ..., d_{k-1}$.

Refer to Figure 5.4 for a visualization of the rule set.

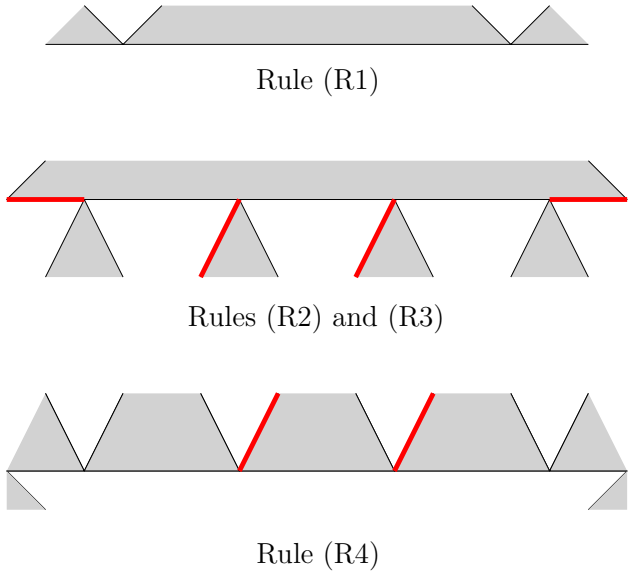

Figure 5.4: Visualization of the rule set from Construction 5.9. Picked segments are highlighted in red.

Next, we verify that the constructed set is a planarization edge set.

Lemma 5.10: *Let $G = (V, E)$ be an optimal 1-planar graph, Q its planar skeleton, R and B the color classes of a proper 2-coloring of Q, $G_B = G[B]$, and T a minimal triangle representation of G_B.*

Then the set P from Construction 5.9 is a planarization edge set of G.

Proof. Recall that as G is TQ-embedded, P is a planarization edge set if and only if it hits all 4-faces of Q by Lemma 2.31. Each 4-face of Q corresponds to a contact point of T, thus we need to show that the rule set picks at least one incident segment for each contact point of T.

Consider a contact point p of T. We do case distinction based on the type of p.

Case 1: p is not horizontal

The point p lies at the end of the base of exactly one primal triangle t (see Figure 2.6). As p is not horizontal, rule (R1) does not apply to t. Thus, rule (R2) picks a segment of the base of t incident to p.

Case 2: p is primal-horizontal

Let t_1 be the upper primal triangle and t_2 the lower primal triangle incident to p. The point p lies on the interior of the base of t_1. (R1) does not apply to t_1, because t_2 touches the base of t_1 at the point p. If t_2 is the leftmost or rightmost primal triangle touching the interior of the base of t_1, then one of the outermost segments of the base of t_1 is incident to p. In that case, rule (R2) applied to t_1 picks a segment incident to p. Otherwise, rule (R3) applied to t_1 picks a segment of t_2 incident to p (see Figure 5.4).

Case 3: p is dual-horizontal

The point p lies at the end of the bases of two primal triangles t_1 and t_2. Let p_1 and p_2 be the endpoints opposite of p of the bases of t_1 and t_2, respectively. If p_1 or p_2 is not horizontal, or if a primal triangle touches the base of t_1 or t_2, then rule (R1) does not apply to both t_1 and t_2. Thus, rule (R2) applies to t_1 or t_2 and picks a segment incident to p.

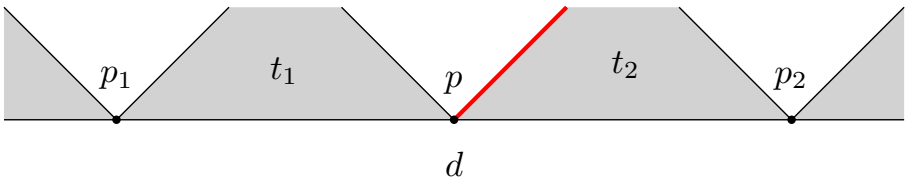

Figure 5.5: Dual-horizontal point where rule (R1) applies to both incident primal triangles.

Otherwise, the bases of t_1 and t_2 form a horizontal line that no primal triangle touches from below. Thus, the line belongs to the base of a single dual triangle d. At p, p_1, and p_2, the tips of other dual triangles touch the interior of the base of d. As p lies in the middle of the three points, rule (R4) applied to d picks a segment incident to p (see Figure 5.5).

■

Next, we verify that the constructed planarization edge set is clustered.

Lemma 5.11: *Let $G = (V, E)$ be an optimal 1-planar graph, Q its planar skeleton, R and B the color classes of a proper 2-coloring of Q, $G_B = G[B]$, and T a minimal triangle representation of G_B.*

Then the planarization edge set P from Construction 5.9 is 10-clustered.

Proof. Our goal is to show that all connected components of $G_P = (V, P)$ contain at most 10 vertices.

First, we analyze the edges corresponding to horizontal segments in T. Let $P_H \subseteq P$ be the set of picked edges corresponding to horizontal segments in T. We show that all connected components of $G_H = (V, P_H)$ contain at most four vertices. Let C_H be the set of triangles in T representing the vertices of a connected component of G_H.

We observe that each picked horizontal segment is an outermost segment for the base of both incident triangles. For primal triangles, this immediately follows from the rule set. For each dual triangle d with at least three segments along its base, consider a non-outermost segment s. The primal triangle t above s has horizontal points at both ends of its base, and no primal triangle's tip touches the base of t. Thus, by rule (R1), we pick no horizontal segment for t (see Figure 5.4).

From the fact that all picked horizontal segments are outermost segments, it follows that each triangle has at most two picked horizontal segments. Furthermore, the bases of all triangles in C_H have their base along the same horizontal line. That leaves four cases for how two adjacent triangles of C_H can lie in T:

(1) The leftmost segments of both triangles align. Then C_H can only continue to the right. Thus, this case happens at most once in C_H.

(2) The rightmost segments of both triangles align. Then C_H can only continue to the left. Thus, this case happens at most once in C_H.

(3) The leftmost segment of the primal triangle aligns with the rightmost segment of the dual triangle. This case can be ruled out as it forms a counterclockwise cycle in T.

(4) The rightmost segment of the primal triangle aligns with the leftmost segment of the dual triangle. Only case (3) can connect multiple instances of case (4). As we ruled case (3) out, case (4) can happen at most once in C_H.

Thus, C_H contains no more than four triangles. Refer to Figure 5.6 for a visualization.

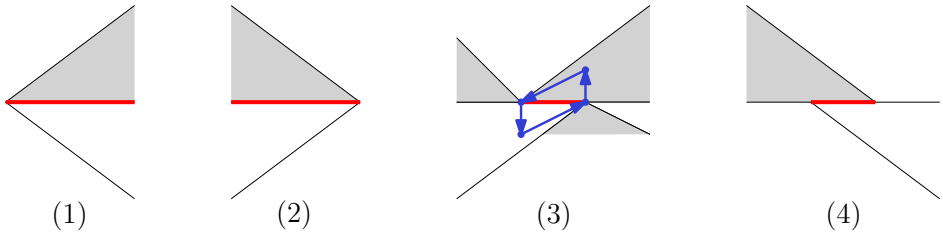

Figure 5.6: Types of picked horizontal segments. In type (3), the counterclockwise cycle of the triangle representation is highlighted.

Next, we analyze the edges corresponding to non-horizontal segments in T. Let $P_N \subseteq P$ be the set of edges corresponding to picked non-horizontal segments in T. We show that all connected components of $G_N = (V, P_N)$ contain at most three vertices.

We observe that we only pick non-horizontal segments on the left side of primal triangles and on the right side of dual triangles. Furthermore, we only pick non-horizontal segments if they are incident to a horizontal point. Thus, all picked non-horizontal segments are outermost segments of the non-horizontal sides of both incident triangles. It follows that we pick at most two non-horizontal segments per triangle.

We also observe that if we pick two non-horizontal segments of a triangle t, we pick one segment via rule (R3) and one via rule (R4). In this case, the side of t ends in two horizontal points. Therefore, all triangles neighboring t on that side have only a single segment on their side touching t, see Figure 5.7. In particular, they have at most one picked non-horizontal segment. It follows that connected components of G_N contain at most three vertices.

Next, we analyze how the connected components of G_N interact with the edges in P_H. Our goal is to show that all connected components of G_N contain at most one vertex incident to an edge from P_H.

If we pick a non-horizontal segment s on the side of a primal triangle t_1 and a dual triangle d via rule (R3), then d has no picked horizontal segment: The tip of t_1 is not the leftmost tip touching the base of the above primal triangle t_2. Thus, the base of d is a segment of the base of t_2, and that segment is not an outermost segment of the base of t_2. Thus, we pick no horizontal segment of d.

If we pick a non-horizontal segment on the side of a primal triangle t via rule (R4), then rule (R1) applies to t, and therefore t has no picked horizontal segment.

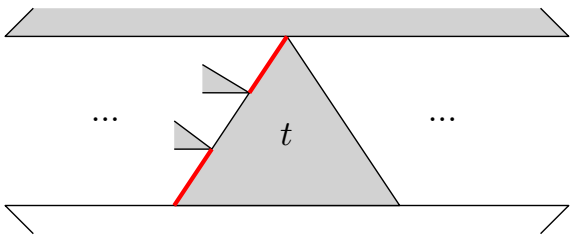

Figure 5.7: Example of a primal triangle with two picked left segments in Construction 5.9. The right sides of the dual triangles touching the left side of t only have one segment.

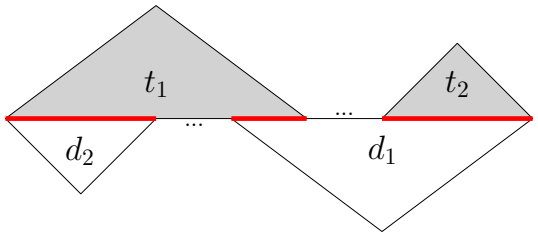

Figure 5.8: Maximum component formed by picked horizontal segments in Construction 5.9.

For components of G_N of size two, it immediately follows that at most one of its vertices has an incident edge in P_H. A component of G_N of size three contains a vertex represented by a triangle t with two picked non-horizontal segments. As we pick one of these segments via rule (R3) and one via rule (R4), both t and one of its neighbors in the component have no picked horizontal segment.

Thus, edges in P_N do not form connections between components of G_H. Therefore, we can think of all components of G_P with at least four vertices as a path in G_H with additional disjoint paths of length one or two attached via edges from P_N. This immediately yields a component size of at most 12 for G_P. We further improve this bound to 10.

Let C be a connected component of G_P. Observe that if C contains at least 10 vertices, C contains a path X from G_H such that X visits four vertices. Together, the triangles representing X in T have a picked segment of each of the types (1), (2), and (4). Let t_1 be the primal triangle, and d_1 be the dual triangle sharing the picked segment of type (4). Let d_2 be the dual triangle sharing the picked segment of type (1) with t_1. Let t_2 be the primal triangle sharing the picked segment of type (2) with d_1. Refer to Figure 5.8 for a visualization.

If t_2 or d_2 has no picked non-horizontal segment, then C contains at most 10 vertices.

Consider the case where t_2 and d_2 both have a picked non-horizontal segment. Let d_3 and t_3 be the triangles connected to t_2 and d_2 respectively via the picked non-horizontal segment

The point p at the right corner of d_2 is primal-horizontal because t_1 has a segment of type (4). The point p is the leftmost point where another primal triangle's tip touches the interior of the base of t_1. Therefore, we do not pick the non-horizontal segment of d_2 via rule (R3), so we pick it via rule (R4). Thus, the tip of d_2 is a horizontal point. Therefore, the left side of t_3 is a subset of the right side of d_2. Thus, t_3 has at most one picked non-horizontal segment and is therefore a leaf. Analogously, d_3 is a leaf. Thus, C contains at most 10 vertices.

The upper bound of 10 for the component sizes of G_P is tight. Figure 5.9 shows a component of size 10 formed by the segments picked in Construction 5.9. ∎

Finally, we obtain Theorem 5.2 as a corollary of Lemmas 3.4, 5.10, and 5.11.

5.2 On Generalizing Theorem 5.2

In Theorem 4.14, we present a reduction from all TQ-embedded graphs to those with a planar skeleton that has no separating triangles. Attempting to generalize Theorem 5.2 to all optimal 1-planar graphs in a similar way suggests itself.

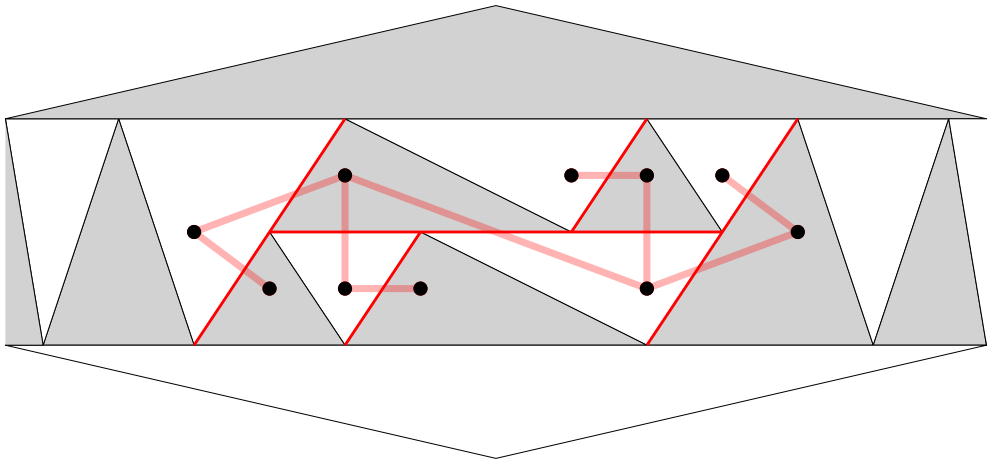

Figure 5.9: Maximum component formed by picked segments in Construction 5.9.

Recall that in Section 4.2, for our TQ-embedded graph G, we pick an inclusion-minimal separating triangle T in the planar skeleton, obtain a planarization edge set P for $G - \text{ext}(T)$ from our premise, modify it to contain no edges incident to T, and then merge P with a planarization edge set of $G - \text{int}(T)$ we obtain from induction.

In an analogous approach to eliminating separating 4-cycles in the planar skeleton of optimal 1-planar graphs, we encounter the following issue. Let G be the embedded optimal 1-planar graph with the planar skeleton Q depicted in Figure 5.10. Consider the highlighted separating 4-cycle C of Q. The graph $Q - \text{int}(C)$ is not 3-connected. Therefore, the graph obtained from $Q - \text{int}(C)$ by adding a pair of crossing edges to each 4-face is not simple, which prevents us from calling induction on $Q - \text{int}(C)$.

Choosing a larger separating 4-cycle so that $Q - \text{int}(C)$ is 3-connected creates another issue. Consider the separating 4-cycle D in Q that encloses $\text{int}(C)$ and the face f. The boundary of f contains three of the four vertices of D. Thus, it is not possible to find a planarization edge set for $G - \text{ext}(D)$ that hits f and contains no edge incident to any vertex of D.

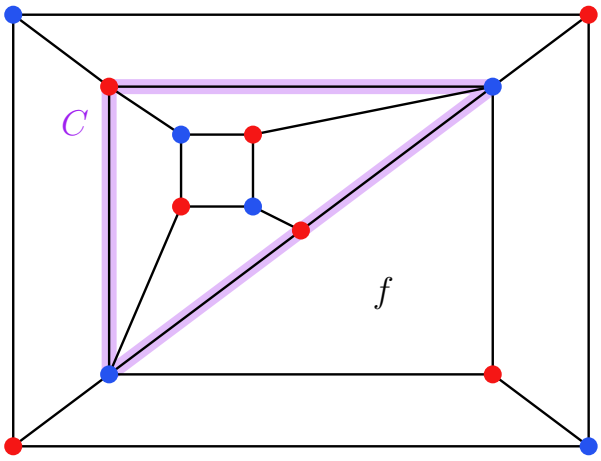

Figure 5.10: Planar skeleton of an optimal 1-planar graph for which our approach for eliminating separating 4-cycles does not work.

6 Conclusion

In this thesis, we mainly investigate the question of whether all 1-planar graphs admit a 4-coloring with bounded clustering. We investigate approaches based on finding planarization edge sets.

Unfortunately, we do not arrive at a conclusive answer to our main research question. However, we answer it affirmatively for the special case of optimal 1-planar graphs without separating 4-cycles in the planar skeleton. As the approach we discuss for generalizing this result to all optimal 1-planar graphs does not succeed, further research attempting this generalization is of interest.

In our research on clustered colorings of general 1-planar graphs, we introduce TQ-embedded graphs. TQ-embedded graphs let us reduce the problem of finding planarization edge sets to a class of graphs with strong and intuitive structural properties. Thus, further research into TQ-embedded graphs and their planarization edge sets would be helpful to better understand and potentially resolve difficulties in finding clustered planarization edge sets.

In our own approaches towards finding clustered planarization edge sets of TQ-embedded graphs, a recurring problem lies in avoiding paths of arbitrary length. While we present a simple way to avoid stars of arbitrary size in general TQ-embedded graphs with our approach based on the primal-dual triangle representation, we only manage to avoid long paths for two special cases.

In our result on optimal 1-planar graphs, we use the intricate notion of a minimal triangle representation. Our other construction managing to avoid long paths is restricted to the very limited class of TQ-embedded graphs with a planar skeleton that admits a representation as a horizontally domino-covered grid. Even for domino-covered grids where both horizontally and vertically adjacent cells may be fused, we do not find a construction for a planarization edge set avoiding long paths.

Therefore, we believe research on planarization edge sets that avoid long paths to be the most important step towards answering whether all TQ-embedded graphs admit a clustered planarization edge set.

It is possible that not all TQ-embedded graphs admit a planarization edge set with bounded clustering, even if all 1-planar graphs admit a 4-coloring with bounded clustering. Other approaches for constructing clustered 4-colorings may be more fruitful. Our inductive reduction to TQ-embedded graphs is not applicable to clustered 4-colorability directly because we do not know how to reconcile non-isomorphic colorings of our separator. However, it may be possible to apply a similar reduction to other approaches for constructing clustered 4-colorings, depending on the degree of control they provide over the produced colorings.

Bibliography

[AC96] Michael O. Albertson and Karen L. Collins. “Symmetry Breaking in Graphs”. In: *The Electronic Journal of Combinatorics* Volume 3 (June 1996). DOI: *10.37236/1242*.

[Ack20] Eyal Ackerman. “Quasi-planar Graphs”. In: *Beyond Planar Graphs: Communications of NII Shonan Meetings*. Singapore: Springer Singapore, 2020, pp. 31–45. DOI: *10.1007/978-981-15-6533-5_3*.

[AH77] K. Appel and W. Haken. “Every planar map is four colorable. Part I: Discharging”. In: *Illinois Journal of Mathematics* Volume 21 (1977), pp. 429–490. DOI: *10.1215/ijm/1256049011*.

[AHK77] K. Appel, W. Haken, and J. Koch. “Every planar map is four colorable. Part II: Reducibility”. In: *Illinois Journal of Mathematics* Volume 21 (1977), pp. 491–567. DOI: *10.1215/ijm/1256049012*.

[Bek20] Michael A. Bekos. “k-Planar Graphs”. In: *Beyond Planar Graphs: Communications of NII Shonan Meetings*. Singapore: Springer Singapore, 2020, pp. 109–130. DOI: *10.1007/978-981-15-6533-5_7*.

[BG20] Michael A. Bekos and Luca Grilli. “Fan-Planar Graphs”. In: *Beyond Planar Graphs: Communications of NII Shonan Meetings*. Singapore: Springer Singapore, 2020, pp. 131–148. DOI: *10.1007/978-981-15-6533-5_8*.

[Bin+15] Carla Binucci, Emilio Di Giacomo, Walter Didimo, Fabrizio Montecchiani, Maurizio Patrignani, Antonios Symvonis, and Ioannis G. Tollis. “Fan-planarity: Properties and complexity”. In: *Theoretical Computer Science* Volume 589 (2015), pp. 76–86. DOI: *10.1016/j.tcs.2015.04.020*.

[Bor84] Oleg V. Borodin. “Solution of Ringel’s problems on vertex-face coloring of plane graphs and coloring of 1-planar graphs”. In: *Met Diskret Anal (in Russian)* Volume 41 (1984), p. 12.

[Bor95] Oleg V. Borodin. “A new proof of the 6 color theorem”. In: *Journal of Graph Theory* Volume 19 (1995), pp. 507–521. DOI: *10.1002/jgt.3190190406*.

[BSV99] P. Boiron, E. Sopena, and L. Vignal. “Acrylic improper colorings of graphs”. In: *Journal of Graph Theory* Volume 32 (1999), pp. 97–107. DOI: *10.1002/(SICI)1097-0118(199909)32:1<97::AID-JGT9>3.0.CO;2-O*.

[CH13] Július Czap and Dávid Hudák. “On Drawings and Decompositions of 1-Planar Graphs”. In: *The Electronic Journal of Combinatorics* Volume 20 (June 2013). DOI: *10.37236/2392*.

[CSY19] Yanan Chu, Lei Sun, and Jun Yue. “Note on improper coloring of 1-planar graphs”. In: *Czechoslovak Mathematical Journal* Volume 69 (2019), pp. 955–968. DOI: *10.21136/CMJ.2019.0558-17*.

[Ead+13] Peter Eades, Seok-Hee Hong, Naoki Katoh, Giuseppe Liotta, Pascal Schweitzer, and Yusuke Suzuki. "A linear time algorithm for testing maximal 1-planarity of graphs with a rotation system". In: *Theoretical Computer Science* Volume 513 (2013), pp. 65–76. ISSN: 0304-3975. DOI: *https://doi.org/10.1016/j.tcs.2013.09.029*.

[Fel01] Stefan Felsner. "Convex Drawings of Planar Graphs and the Order Dimension of 3-Polytopes". In: *Order* Volume 18 (2001), pp. 19–37. DOI: *10.1023/A:1010604726900*.

[Fel04] Stefan Felsner. "Lattice Structures from Planar Graphs". In: *The Electronic Journal of Combinatorics* Volume 11 (Feb. 2004). DOI: *10.37236/1768*.

[FG54] F.G. "Tinting Maps". In: *The Athenaeum* (June 1854), p. 726. URL: *https://books.google.de/books?id=Mm1IAAAAYAAJ&pg=PA726* (visited on 03/16/2026).

[GB07] Alexander Grigoriev and Hans L. Bodlaender. "Algorithms for Graphs Embeddable with Few Crossings per Edge". In: *Algorithmica* Volume 49 (2007), pp. 1–11. DOI: *10.1007/s00453-007-0010-x*.

[GLP12] Daniel Gonçalves, Benjamin Lévêque, and Alexandre Pinlou. "Triangle Contact Representations and Duality". In: *Discrete & Computational Geometry* Volume 48 (2012), pp. 239–254. DOI: *10.1007/s00454-012-9400-1*.

[GT95] Ashim Garg and Roberto Tamassia. "Upward planarity testing". In: *Order* Volume 12 (1995), pp. 109–133. DOI: *10.1007/BF01108622*.

[He93] Xin He. "On Finding the Rectangular Duals of Planar Triangular Graphs". In: *SIAM Journal on Computing* Volume 22 (1993), pp. 1218–1226. DOI: *10.1137/0222072*.

[Hon20] Seok-Hee Hong. "Beyond Planar Graphs: Introduction". In: *Beyond Planar Graphs: Communications of NII Shonan Meetings*. Singapore: Springer Singapore, 2020, pp. 1–9. DOI: *10.1007/978-981-15-6533-5_1*.

[JLR15] Konstanty Junosza-Szaniawski, Mathieu Liedloff, and Paweł Rzążewski. "Fixing Improper Colorings of Graphs". In: *SOFSEM 2015: Theory and Practice of Computer Science*. Berlin, Heidelberg: Springer Berlin Heidelberg, 2015, pp. 266–276. DOI: *10.1007/978-3-662-46078-8_22*.

[Kan08] Ross J. Kang. "Improper colourings of graphs". PhD thesis, University of Oxford, 2008. URL: *https://ora.ox.ac.uk/objects/uuid:a93d8303-0eeb-4d01-9b77-364113b81a63*.

[KK85] Krzysztof Koźmiński and Edwin Kinnen. "Rectangular duals of planar graphs". In: *Networks* Volume 15 (1985), pp. 145–157. DOI: *10.1002/net.3230150202*.

[KU22] Michael Kaufmann and Torsten Ueckerdt. "The Density of Fan-Planar Graphs". In: *The Electronic Journal of Combinatorics* Volume 29 (Feb. 2022). DOI: *10.37236/10521*.

[LW22] Chun-Hung Liu and David R. Wood. *Clustered Graph Coloring and Layered Treewidth*. Version 4. Sept. 2022. DOI: *arXiv:1905.08969v4*.

[MS25] Laura Merker and Samuel Schneider. *Algorithmic Graph Theory – Problem Class 1*. Class at Karlsruhe Institute of Technology. 2025. URL: *https://i11www.iti.kit.edu/_media/teaching/sommer2025/problem_session_1.pdf* (visited on 02/11/2026).

[PSS96] J. Pach, F. Shahrokhi, and M. Szegedy. "Applications of the crossing number". In: *Algorithmica* Volume 16 (1996), pp. 111–117. DOI: *10.1007/BF02086610*. URL: *https://doi.org/10.1007/BF02086610*.

[PT97] János Pach and Géza Tóth. "Graphs drawn with few crossings per edge". In: *Combinatorica* Volume 17 (1997), pp. 427–439. DOI: *10.1007/BF01215922*.

[Rin65] Gerhard Ringel. “Ein Sechsfarbenproblem auf der Kugel”. In: *Abhandlungen aus dem Mathematischen Seminar der Universität Hamburg* Volume 29 (1965), pp. 107–117. DOI: *10.1007/BF02996313*.

[Riv93] Ivan Rival. “Reading, Drawing, and Order”. In: *Algebras and Orders*. Springer Netherlands, 1993, pp. 359–404. ISBN: 978-94-017-0697-1. DOI: *10.1007/978-94-017-0697-1_9*.

[Sch89] Walter Schnyder. “Planar graphs and poset dimension”. In: *Order* Volume 5 (1989), pp. 323–343. DOI: *10.1007/BF00353652*.

[SS23] Lili Song and Lei Sun. “1-planar graphs with girth at least 6 are (1,1,1,1)-colorable”. In: *Czechoslovak Mathematical Journal* Volume 73 (2023), pp. 993–1006. DOI: *10.21136/CMJ.2023.0418-21*.

[Suz10] Yusuke Suzuki. “Re-embeddings of Maximum 1-Planar Graphs”. In: *SIAM Journal on Discrete Mathematics* Volume 24 (2010), pp. 1527–1540. DOI: *10.1137/090746835*.

[Suz20] Yusuke Suzuki. “1-Planar Graphs”. In: *Beyond Planar Graphs: Communications of NII Shonan Meetings*. Singapore: Springer Singapore, 2020, pp. 47–68. ISBN: 978-981-15-6533-5. DOI: *10.1007/978-981-15-6533-5_4*.

[Uec] Torsten Ueckerdt. Private communication.

[Whi31] Hassler Whitney. “A Theorem on Graphs”. In: *Annals of Mathematics* Volume 32 (1931), pp. 378–390. DOI: *10.2307/1968197*.

[Woo18] David Wood. “Defective and Clustered Graph Colouring”. Version DS23. In: *The Electronic Journal of Combinatorics* (Apr. 2018). DOI: *10.37236/7406*.